理學碩士 學位論文

수소화물 기상 에피탁시법을 이용한 자립형 GaN 박막 성장에 관한 연구

Hydride Vapor Phase Epitaxy of Freestanding GaN Films

2010年 2月

韓國海洋大學校 大學院

應用科學科 半導體物理專攻

金 是 永

理學碩士 學位論文

수소화물 기상 에피탁시법을 이용한 자립형 GaN 박막 성장에 관한 연구

Hydride Vapor Phase Epitaxy of Freestanding GaN Films

指 導 敎 授　張 志 豪

2010年 2月

韓國海洋大學校 大學院

應用科學科　半導體物理專攻

金 是 永

本 論文을 金是永의 理學碩士 學位論文으로 認准함

위원장　李 三 寧 (인)

위 원　安 亨 秀 (인)

위 원　張 志 豪 (인)

2010 년 2 월

한국해양대학교 대학원

Contents

Chapter 1. Introduction

1.1) Introduction to III-Nitrides semiconductors

1.2) Necessity of Free-standing GaN substrate

Chapter 2. Experimental

2.1) growth method

Chapter 3. Comparison of GaN on Zn-polar/O-polar ZnO

Chapter 4. Optimization of growth condition for high quality GaN grown on ZnO template

논 문 요 약

본 논문에서는 III-V족 화합물 반도체인 GaN 물질을 ZnO를 template 층을 이용하여 Sapphire 기판 위에 성장하였고 구조적, 광학적 조사를 통하여 고품질의 Freestanding(FS)-GaN 기판의 제작에 대한 가능성을 고찰하였다. 이 논문의 목적은 종래에 사용해 오던 기판 제거 방법의 문제점들에 의해 고품질의 성장이 제한이 되어온 것에 대하여 GaN 기판을 ZnO를 sacrificial 층으로 사용, 성장 조건의 최적화에 따른 FS-GaN 기판의 새로운 성장 가능성을 보여줌에 있다. 본 논문은 총 6 장으로 구성되어 있으며 각 장의 내용은 다음과 같다.

제 1장에서는 기본적인 GaN 물성과 종래의 FS-GaN 기판제작이 가지고 있는 문제점, 그리고 다양한 응용분야에 대하여 설명을 하였다. 제 2장에서는 제작된 자립형 GaN 기판을 성장, 평가하기 위해 본 연구에서 사용한 방법인 HVPE, SEM, HRXRD 그리고 PL 측정에 대하여 정리를 하였다. 제 3장은 GaN의 성장을 위한 ZnO template 층의 적합한 polarity의 확인에 있다. 다른 polarity를 가지는 ZnO 위에 성장된 GaN의 구조적 및 광학적 특성에 대해 고찰 하였다. 제 4장에서는 성장온도 및 가스 flow (V/III)의 변화를 통하여 GaN 성장에 적합한 성장조건을 구조적 및 광학

적 특성 평가를 통하여 확인하였다. 그리고 제 5장에서 3장과 4장에서 확인 된 ZnO의 polarity와 GaN의 성장조건을 통하여 자립형 GaN 기판을 화학적 etching 방법을 통하여 제작 하였으며 마지막으로 제 6장에서는 본 논문에서 얻은 결과를 정리하여 결론 및 향후 과제에 대해 기술하였다.

Abstract

In this thesis, the growth structural and optical properties of FS-GaN with ZnO template buffer layer have been investigated. The objective of this thesis is to fabricate the high quality FS-GaN substrate by using ZnO sacrificial layer.

In the chapter 1, the fundamental GaN properties, problems in the fabrication of FS-GaN substrate, and many application of the GaN are introduced. In the chapter 2, the principles of hydride vapor phase Epitaxy (HVPE), scanning electron microscopy (SEM), high resolution X-ray diffraction (HR-XRD), and photoluminescence (PL) are explained. In the chapter 3, ZnO polarity was determined for the growth of GaN on ZnO. In the chapter 4, the high quality GaN film growth was achieved by using ZnO sacrificial layer and optimization of growth condition. And in the chapter 5, a new self-separation method by using chemical etching of ZnO template was developed. And the quality of GaN was characterized in terms of structural and luminescence properties. Finally, the results found from this thesis are summarized and concluded in the chapter 6.

Figure list

Chapter 1

Chapter 2

Chapter 3

Chapter 4

6

Chapter 5

Table list

Chapter1. Introduction

1.1) Introduction to III-Nitrides semiconductors

1.1.1) Application of GaN

Epitaxial GaN and its alloys with Al and In are emerging wide-gap semiconductors well suited for the fabrication of semiconductor devices including light emitting diodes and lasers and high power, high temperature and high frequency electronic applications.[1-2] There are two fundamental reasons to choose nitrides for blue-light sources. Foremost is the large bandgap associated with the Al-Ga-In-N system, which encompasses the entire visible spectrum as shown FIG. 1.1 The $Ga_xIn_{1-x}N$ ternary alloys, represented in the FIG. 1.1 by the lower segment of the nitride triangle, have bandgap ranging from 0.65eV ~1.0eV for InN to 3.4eV for GaN.[3-4] The other main advantage of the nitrides over other high-bandgap semiconductors is the strong chemical bond which makes the material very stable and resistant to degradation under conditions of high electric currents and intense light illumination. Furthermore, a great advantage of GaN, InN and AlN materials is that all these direct band gap semiconductors can be

applied to optical devices, which are luminous over the entire visible to ultraviolet

spectrum by making ternary compounds of III-nitrides such as InGaN and AlGaN.

The development of GaN-based optical devices is expected to have an

enormous effect on display and lighting technology.
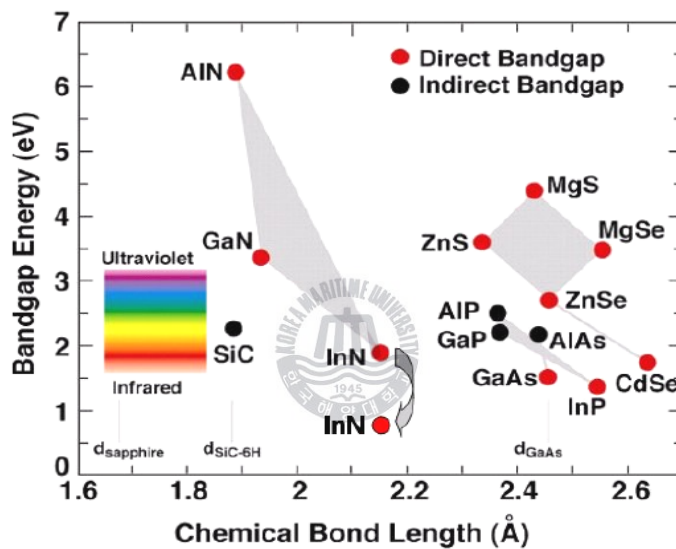
FIGURE 1.1 Bandgap and chemical bond lengths of compound semiconductors that emit in the visible range of the electromagnetic spectrum. The visible spectrum is shown as related to the energy gap of the semiconductors.

GaN-based visible light emitting diodes (LEDs) are already commercialized

for a variety of lighting; the application of blue, green and LEDs is full-color

displays, traffic lights, automotive lighting and general room lighting using white

LEDs. [5] In addition, blue laser diodes (LDs) can be used in high storage-capacity

digital versatile disks (DVDs) system. [6] Green laser diodes can be used in portable laser display. AlGaN-based photo-detectors are also useful for solar-blind UV detection and have applications as flame sensors for control of gas turbines or for detection of missiles. Those GaN-based optical devices will by more widely used due to excellent optical properties of GaN. Moreover, with the recent revision of the band gap of InN at ~0.65eV[3-4], the band gap of the InGaN material system now rages from the infrared to the ultraviolet region.

This direct and wide band gap range makes the InGaN material system useful for photovoltaic applications due to the possibility of fabricating not only high-efficiency multi-junction solar cells based solely on the nitride material system. Detailed balance modeling indicate that in order to achieve practical terrestrial photovoltaic efficiencies of greater than 50%, materials with band gaps greater than 2.4 eV are required [7] addition to the wide band gap range, the nitrides also demonstrate favorable photovoltaic properties such as low effective mass of carriers, high mobilities, high peak and saturation velocities, high absorption coefficients, and radiation tolerance. The III-V nitride technology has demonstrated the ability to grow high-quality crystalline structures and fabricate

optoelectronic devices, which confirms its potential in high-efficiency photo-voltaics.[8]

1.1.2) Physical properties of GaN

TABLE 1.1 Material properties of GaN

Property		Value
RT(300K) energy band gap(eV)		3.44
Lattice constant	a-plane (Å)	3.18843
	c-plane (Å)	5.18524
Density(g/cm^3)		6.15
Coefficient of thermal expansion at 300K	a-axis (10-6/K)	5.59
	c-axis (10-6/K)	3.17
Thermal conductivity at 300K (W/cm·^{0}C)		>2.1
Infrared refractive index		2.3
Electron affinity (eV)		3.4
Elastic constants (GPa)	C11	390±15
	C12	145±20
	C13	106±20
	C33	398±20
	C44	105±10
Heat capacity at 300K (J/mol·K)		35.3
Group of symmetry		C6$_3$*mc*

Gallium nitride and other III-nitrides have particular material properties compared with other III-V materials such as GaAs or InP because the metallic

12

atoms are strongly bonded to very small nitrogen atoms. Gallium (^{31}Ga or Ga) and Nitrogen (^{7}N or N) form *sp3* hybrid orbital among the nearest atoms, and N has a very small atomic and ionic radii; electrons are very strongly bonded to the nucleus. Consequently, GaN has ionic as well as covalent bonds and very short and strong bonds. This is closely related to why GaN has a high melting point, thermal and chemical stability, wide band-gap and high thermal conductivity as shown in

TABLE 1.1 this table shows a summery of the physical properties of GaN.

1.1.3) Problems in GaN Epitaxy

Although GaN itself is the best choice as a substrate for GaN epitaxy and device fabrication, commercialization of FS GaN substrate need more times. There are many difficulties and problems in fabrication of FS GaN substrate because of high equilibrium vapor pressure of nitrogen in GaN and high melting point of GaN.

Phase diagram of FIG. 1.2 showed that, at pressures above 6 GPa, congruent melting of GaN happened at about $2,220^{0}$C, and to decrease the temperature allowed the GaN melt to be crystallized. [9] Thus, it is difficult to grow bulk GaN, and film quality was eventually deteriorated by hetero-epitaxy on foreign

substrates.
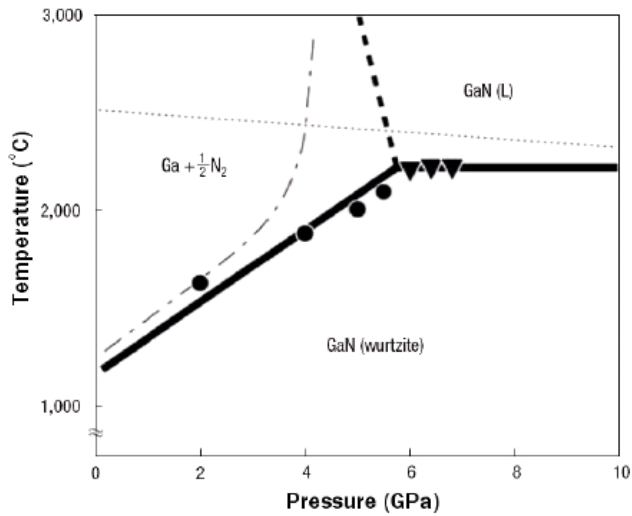
FIGURE 1.2 Phase diagram of GaN. [9]

For these reasons, typically GaN layers are grown on various foreign

substrates such as sapphire (Al_2O_3), SiC and $LiGaO_2$ etc. as shown in TABLE 1.2.

[6] That is, selection of an appropriate substrate is critical. Sapphire, which is the

most commonly used substrate in GaN epitaxial growth, is interesting because this

substrate seems to be unsuitable from the viewpoint of material properties

compared with GaN; sapphire has large lattice misfit over than 16% and thermal

expansion coefficient mismatching with GaN. From these factors, many cracks

were easily generated and only inferior GaN layer with very rough surface

14

morphology was obtained by early GaN research groups. These mismatches between the sapphire substrate and epitaxial GaN layer induce the generation of a high density of dislocation in GaN thin films. Sapphire is the most commonly used substrate for epitaxial growth of the III-nitrides as addressed in before section.

However, the large differences in lattice parameter and in linear thermal expansion rates that occur both within the AlGaInN system itself and relative to sapphire substrates meant that poor-quality epitaxial films were expected. In the search for improved properties, Akasaki and Nakamura suggested that a low temperature (LT) AlN and a LT GaN between sapphire substrate and epitaxial GaN film.[10-11] Although amorphous and therefore not of as high quality as the desired film, the buffer layers allowed for continuous coverage of the substrate and overcame the wetting obstacles related to surface and interface energetics. Aksaki grew the first smooth surfaces of GaN films in 1986, demonstrating that two-dimensional nucleation in nitride Epitaxy could be achieved and thereby bringing about a significant improvement in the electrical and luminescent properties of the films. LT buffer layers have contributed do improve crystallinity, electrical and optical properties of GaN layers. However, there still are many obstacles to realize

15

long lifetime and high power devices.

TABLE 1.2 Material properties of substrates for GaN Epitaxy

Crystal	Structure	Lattice misfit [%]	TEC mismatch [%]	Price (c-plane) 10 x 10 mm ($)
GaN	Wurtzite	0	0	1295
AlN	Wurtzite	3	33	
Sapphire (Al$_2$O$_3$)	Corundum	16	-25	5
SiC (6H)	6H Wurtzite	4	24	220
Si	Diamond	-17	115	
GaAs	Zincblende	-20	-7	
LiAlO$_2$	Orthorhombic	-1	-21	54
LiGaO$_2$	Orthorhombic	1	-23	65
ZnO	Wurtzite	-2	-13	140

The misfit dislocation act as nonradiative recombination centers and reduce

the quantum efficiency.[12] More important problem in a GaN based devices is

breakdown or failure during operation. The operation of device is strongly

influenced by junction temperature of active-region. Breakdown or failure of

devices occurs in defect area such as nanopipes and threading dislocation (TD),

when heat occurs to device during operation.[13] By such reasons, other buffer

layer such as ZnO, InN as well as LT-AlN and LT-GaN were suggested as useful

technique to get GaN films with low dislocation density.[14-15] Despite a lot of

16

buffer layers have been tried, many TDs that extend along the c-axis of grown GaN films from the interface between the substrate and epitaxial layer.

1.1.4) Piezoelectric polarization in GaN

It is relatively easy to grow planar c-plane GaN due to its large growth stability. Nearly all wurtzite III-nitride-based devices have been grown predominantly in the (0001) or c-plane orientation. However, owing to their P63mc symmetry, wurtzite structures are polar. Since the wurtzite structure has polar symmetry, the material has a spontaneous polarization in the polar axis parallel to c-<0001> direction. The addition of strain causes piezoelectric polarization, which is much larger in value and might be either on the same or the opposite direction of the spontaneous polarization. Following FIG 1.3 exhibits the effect of strain and the growth face on the direction of the spontaneous and piezoelectric polarization. Piezoelectric field is induced since group III-nitride have large piezoelectric constants along c-<0001> direction.

As can be seen from FIG 1.3, if i grown on different faces either Ga-(0001) face or N-(000-1) face, i seen opposite effects. [16]
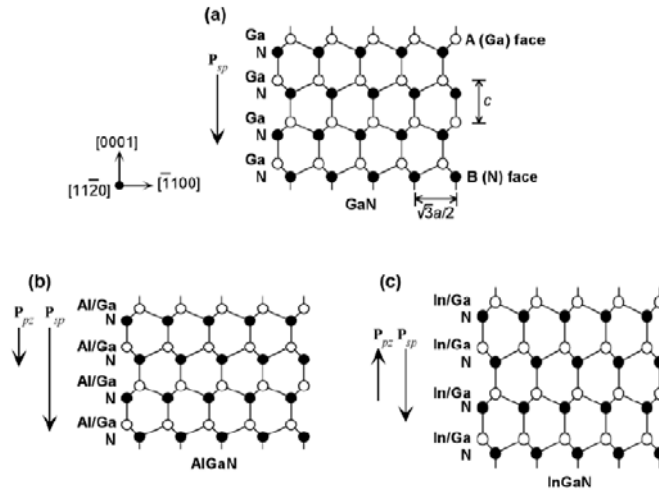
FIGURE 1.3 schematic diagram of crystal structure and of the spontaneous and piezoelectric polarization fields present in (a) unstrained GaN; (b) The lattice constants a and c and the A (Ga-terminated) (a) and B (N-terminated) crystal faces are indicated for GaN.[16]

As a result of the piezoelectric and spontaneous polarizations the optical properties of III-nitrides are strongly affected by the quantum confined Stark effect (QCSE) as demonstrated in FIG 1.3, leading to shift in emission wavelength and decrease in intensity. Polarization fields cause the device to perform inefficiently due to poor electron-hole recombination resulting from electron-hole separation. In FIG. 1.4 it is shown that the electron and hole wave-functions are separated and pushed toward the opposite sides of the well.
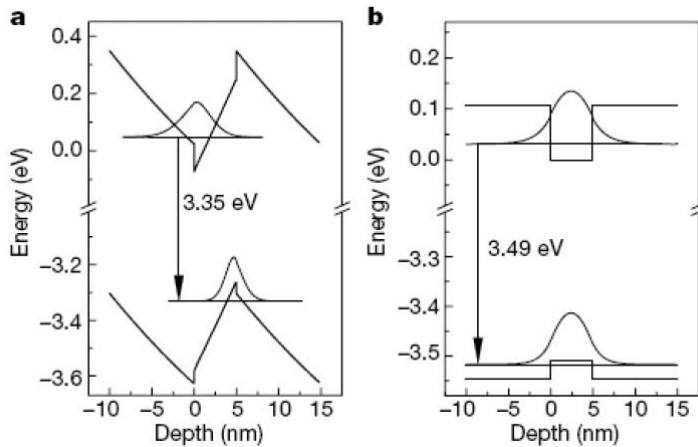
FIGURE 1.4 A comparison on between a) polar c-plane GaN/AlGaN SQW band diagram in the presence of polarization electric and b) m- or a-plane GaN/AlGaN SQW band diagram in the absence of PE.[17]

The reduced overlap results in a corresponding reduction in radiative recombination rates. The probability of carriers tunneling out of the well also increases, resulting in a decrease in carrier lifetimes and broadening of the absorption spectra. As a result, optical transitions are less intense, and red-shifted.

1.2) Necessity of Free standing GaN substrate

1.2.1) History of GaN substrates and problems of fabrication

Basically, there are many difficulties and problems in fabrication of bulk GaN because of high equilibrium vapor pressure of nitrogen in GaN and high melting point of GaN. Phase diagram of FIG. 1.2 showed that, at pressures above 6

GPa, congruent melting of GaN happened at about 2,220^{0}C, and to decrease the

temperature allowed the GaN melt to be crystallized.[18] By these reasons,

although bulk GaN growth technique has been researched for a long time, these

methods have not produced a bulk GaN ingot.[19-24] In addition, these methods

are less practical for commercial bulk GaN growth owing to limited scalability.

TABLE 1.3 Growth condition and property of bulk GaN

Technique	Substrate (Technique)	Pressure (atm)	Growth temp. (^{0}C)	Growth rate (um/hr)	TD density (/cm^2)	Ref. No
N2 high Pressure		>10,000	>1500	100 (platelet)	<10^4	[19]
Na-flux		<50	600~800	10 (platelet)	~10^6	[20, 21]
Liquid Phase Epitaxy (LPE)	GaN/Sapphre (MOCVD)	9.5	~800	4	10^4~10^5	[22.23]
Ammonothermal	GaN substrate (HVPE)	1900	600~700	~2 (50μm/day)	<10^6	[24.25]

TABLE 1.3 shows a property of grown bulk GaN by N$_2$ high pressure, Na-

flux, liquid phase epitaxy (LPE) and ammonothermal technique. However, the

growth of GaN crystals with extremely low dislocations has been successfully

achieved by the N$_2$ high-pressure growth method, in which the growth of GaN

proceeds in Ga melt. [19] However, the N$_2$ high-pressure growth method has some

disadvantages in its application to industrial use, such as its necessity for

extremely high nitrogen pressure (more than 10,000atm) and high growth temperature (more than 1,500^{0}C) and its relatively low growth rate.

The development of the Na-flux method could lower the required pressure to grow the GaN single crystals in a solution system.[20-21] In this method, the addition of Na to Ga melt promotes nitrogen dissolution, which results in the low pressure (about 50atm) growth of GaN single crystals in Ga-based solution. However, the Na flux method also involves the following problems; 1) Crystals grown by this method are easily colored; 2) Growth rate is low, making it difficult to grow large-size crystals; 3) Nucleation frequency in solution is high. There is very similar method named LPE with Na-flux.[22-23] Compare with Na-flux method, LPE used GaN template grown by MOCVD. So, LPE technique is useful in growth of larger area, but problem in growth rate remains yet. Hydrothermal growth (high-pressure water solution) of quartz is extremely cost effective; 1 million tons of high-quality quartz has been successfully grown by this technique each year. Ammonia is a closer match to the physical properties of water than any other known solvent, and as a nitrogen-based solution, it should be also able to produce many nitrogen-based compounds (i.e. nitrides).[24] Growth of bulk III-

nitride crystals by ammothermal method has several advantages over other growth techniques; (1) simple equipment, (2) process scalability, (3) simultaneous growth on multiple seed, (4) freestanding high-quality single crystal, (5) lower process temperatures compared with other bulk GaN growth techniques. However, growth technology of bulk GaN that use ammothermal methods was studied for about 10 years. But, up to now, in spite of that use expensive GaN substrate by seed, do not pass over 50μm per day in growth rate.

1.2.2) Difficulty in substrate removal technique by HVPE

Enormous effort has been spent in growing single crystal GaN substrates. Several methods for preparing bulk GaN crystals have been investigated [18-25]. There have been several attempts to prepare bulk GaN crystals such as solution growth under N_2 high pressure and Na-flux. However, the size of GaN crystals obtained in these methods is too small for practical use. Also, up to now, growth rate of ammothermal method is 50μm per a day on GaN substrate, too slow.

A HVPE growth of a thick GaN layer is an alternative and promising approach for obtaining such substrates. This is because of the growth rate in HVPE

has reached as high as 100μm/hr, and a bulk-like GaN with thickness of several

hundred micrometers has been easily obtained on substrate of 2inch area. The

current largest 3inch FS-GaN substrate obtained by growing a thick GaN layer on

a sapphire substrate using HVPE and separating the grown layer from the sapphire

substrate.[32]

In the GaN LD structure, when using a sapphire substrate, it is difficult to

obtain cleaved mirror facets which are used for the cavities of conventional LDs.

In addition, the thermal conductivity of sapphire (0.5 W/cm·K) is not as high as

that of GaN (1.3 W/cm·K) for the heat dissipation generated by the LDs. So, the

LDs grown on pure GaN substrates which are easily cleaved and have a high

thermal conductivity are described. Because of these reason, FS-GaN substrate

was developed by a polishing technology at first in 1998 by S. Nakamura.[26]

TAPBLE 1.4 shows development history of FS-GaN substrate using HVPE.

As well known, removing GaN from the sapphire substrate is difficult because the

sapphire substrate is robust material with a negligible etching rate for any etchant.

For this reason, various attempts such as mechanical polishing, etchable substrate,

laser lift-off (LLO), void-assisted separation (VAS), and facet-controlled epitaxial

lateral overgrowth (FACLEO) have been developed to removing sapphire substrate.

[26-31]

First of all, polishing method is time consuming and GaN layers are often

cracked during polishing. Also, FS-GaN substrate fabricated by wet-etching of Si

wafer is very easy method, but quality of grown GaN on Si is very low due to the

large difference of lattice mismatch between GaN and Si.[34]

TABLE 1.4 Development history of FS-GaN substrate by HVPE

Fabrication technique	Substrate for GaN growth	Developer (year)	Ref
Sapphire polishing	Sapphire	Nicha (1998)	[26]
Chemical etching of Si substrate	Si	Taejon national Univ. (1998)	[27]
Laser lift-off	Sapphire	Technishe Univ. (1990)	[28]
Chemical etching of GaAs substrate	GaAs	Sumitomo (2001)	[29]
Void-Assisted Separation	Sapphire	Hitachi (2003)	[30]
Facet-Controlled Epitaxial Lateral Overgrowth (FCELO)	Sapphire	Sumitomo (2005)	[31]

Kelly et al. demonstrated a LLO technique to separate HVPE grown GaN

layer from sapphire.[28] Wong et al. achieve a LLO technique to separate a 2μm

thick GaN layer which bonded onto support Si Substrate.[33] However, GaN

layers close to the lift-off area, where the laser light irradiates, suffer from

damages due to inhomogeneous temperature rise during LLO process.[35]

Moreover, getting the crack-free, large size FS GaN by the laser lift-off technique

is difficult because of fracturing during laser irradiation.[36]

Compared to a sapphire substrate, a GaAs substrate is advantageous for

device fabrication because it is easy to cleave, to each and to make an ohmic

contact. So, in the case of growing a thick GaN film on GaAs substrate for using of

chemical etching effect, FS-GaN substrate can be obtained by simply etching the

GaAs substrate.[29] But, this process has inherent problems such as decomposition

of GaAs substrate at high temperature for GaN growth and inter-diffusion at a

GaN/GaAs interface. Especially, the as auto-doping from the back-side of the

GaAs substrate was serious problem for the GaN growth.[37]

To solve problems such as cracking by mechanical stress during polishing,

GaN damage from high power laser and as auto-doping from GaAs substrate, VAS

and FACLEO method were developed.

The fabrication process of freestanding GaN wafers by VAS is illustrated in

FIG. 1.5. The process consists of many steps. (a) An undoped 300nm thick GaN

layer was grown on top of a 2-inchg diameter c-face sapphire substrate by

MOVPE. (b) A Ti layer about 20 nm thick was deposited on the GaN layer by

vacuum vapor deposition. (c) The Ti-deposited GaN templates were annealed at 1060 ^{0}C for 30min under a mixture gas flow of $H_2:NH_3 = 4:1$. This annealing converted the Ti layer into a nano-net structure of TiN. Simultaneously, a number of small voids were formed in the metal organic vapor phase epitaxy (MOVPE) grown GaN layer. (d) A GaN layer with a thickness of about 300 μm was then grown on the GaN template by HVPE. (e) The GaN layer was easily separated from the sapphire by a weak force after taking the sample out of the reactor. [38]
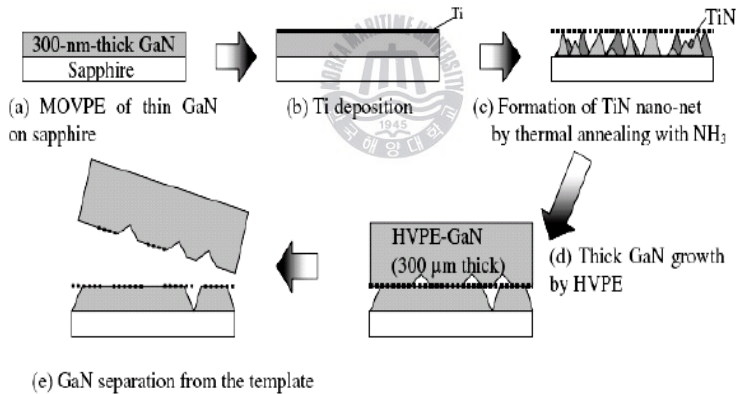
Figure 1.5 Schematic of the VAS process.[38]

Although, VAS technique is very effective method to obtain high quality and large size GaN substrate, this approaches require complex processes such as a deposition of mask materials and a growth of GaN template by MOVPE, prior to the thick-GaN growth by HVPE.

Next, facet controlled epitaxial lateral overgrowth (FACLEO) technique has been developed for the self-separated FS-GaN substrate, as shown in FIG. 1.6. The FACLEO method involves selective area growth (SAG) followed by SiO_2 deposition, which is then followed by re-growth by MOVPE or HVPE, as shown in FIG. 1.6(a). Here, his technique used SAG with GaN such that (11-22) facets form as the GaN grows laterally. The TDs propagating from the underlying GaN are bent horizontally, i.e., toward the <11-20> or <1-100> direction, by inclined facets. After SAG, the side facets are covered by SiO_2 except for the portion of the top, as shown in FIG 1.6 (b).

This terminates most of the TDs. GaN is then grown on an uncovered seed by MOVPE or HVPE, and voids are formed between the masks (FIG. 1.5 (c)). [39] After the GaN HVPE re-growth, 50- to 100-µm-thick layers were separated from the substrate. The separation occurred at the portion of the seeds for re-growth during the cooling of the sample after the HVPE re-growth. A thick GaN layer grown by HVPE can be spontaneously separated from the substrate using the concentration of the compressive stress at the seeds due to the voids formed intentionally.
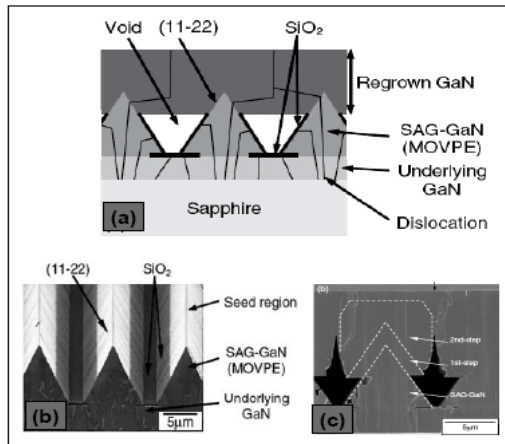
Figure 1.6 Schematic of the FACLEO structure and cross-sectional SEM image of grown GaN by using FACLEO technique.[37]

The fabricated GaN substrate by using FACLEO technique has very high quality due to lateral growth effect. But, this technique has very complex process, such as GaN growth step by MOVPE, SiO$_2$ deposition of two times and photo-lithography of two times, prior to the thick-GaN growth by HVPE.

Conclusively, there are two self-separation methods to obtain GaN substrate by using voided interface structure. These two methods were known as the most progressed method. But, there are a lot of difficulties due to complexity of process.

1.3) Proposal and Purpose of this study

Although freestanding (FS)-GaN substrates grown by hydride vapor phase

epitaxy (HVPE) have been commercialized. Application of FS-GaN to the fabrication of device such as light emitting diodes and laser diodes are progressing slowly. This is mainly because FS-GaN substrates are expensive owing to the difficulty of manufacturing process. Removing of thick GaN layers from the sapphire substrates are difficult because sapphire substrates are robust material with a negligible etching rate for any etchant. For this reason, various attempts such as laser lift-off [26-27], mechanical substrate polishing [28], void-assisted separation (VAS)[29], and facet controlled epitaxial lateral overgrowth (FACLEO)[30] have been developed to remove sapphire substrate[26, 30]. However, the laser lift-off technique has a fracturing problem during laser irradiation [32]. While the other approaches require complex processes such as deposition of mask materials and growth of GaN template prior to growth of the thick-GaN by HVPE. Therefore, recently new approaches are developed like as self-separation of evaporable buffer layer (EBL) [31], and chemical lift-off (Metal-Nitride) [30], but those method requests to surmount several problems comes from the narrow growth window of amorphous (NH_4Cl) layer and different crystal structure of metal-nitride template [30-31]. Therefore, more simple and easy way

29

for the growth and separation of GaN crystal is important especially for the practical point of view. I has proposed a simple self-separation technique by using a sacrificial interlayer made of ZnO that can be easily etched without protecting cover layer in the HVPE process. Because of its similar material properties compared to GaN, ZnO is the ideal candidate for that purpose. Same crystal structure and especially the small lattice mismatch of only about 1.8 % (c-axis) and 0.4% (a-axis), the fact that ZnO can be easily etched makes it very attractive. However the extreme instability of ZnO in the HVPE atmosphere demands a protecting cover layer of GaN before growth [32-33].

Consequently, this study proposed a simple one-step approach of obtaining high quality FS-GaN by using a ZnO sacrificial layer for the direct growth of GaN without protecting cover layer. ZnO template will be easily etched during heating up for HT-GaN growth. Therefore i should check out the growth condition for the fabrication of FS-GaN. And based on the stability of the ZnO with various polarity should be checked out as well. It could be a reliable solution to solve the critical problems of FS-GaN substrate fabrication.

Reference

[1] S. Nakamura, M. Senoh, N. Iwasa and S. Nagahama, Appl. Phys. Lett., 67 (13), 1868 (1995),

[2] H. Amano, N. Sawaki, I. Akasaki and Y. Toyoda., Appl. Phys. Lett., 48 (5), 353 (1986)

[3] F. A. Ponce and D. P. Bour, NATURE, 386, 351 (1997)

[4] T. Matsuoka, H. Okamoto, M. Nakao, H. Harima and E. Kurimoto, Appl, Phys. Lett., 81(7), 1246 (2002)

[5] S. Nakamura, M. Senoh, N. Iwasa, S. Nagahama, T. Yamada and T. Matsushita, H. Kiyoku and Y. Sugimoto, Jpn. J. Appl. Phys. 35, L74 (1996)

[6] A. De Vos, Endoreversible Thermodynamics of Solar Energy Conversion {Oxford Iniversity Press, Oxford, 1992}. P.90

[7] O. Jani, I. Ferguson, C. Honsberg and S. Kurtz, Appl. Phys. Lett., 91, 132117 (2007)

[8] W. Utsumi, H. Saitoh, H. Kaneko, T. Watanuki, K. Aoki   and I. Shimomura, Natue Materials, 2, 735 (2003)

[9] H. Amano, N. Sawaki, I. Akasaki and T. Yoyoda, Appl. Phys. Lett. 48. 353 (1986),

[10] Y.S. Nakamura, M. Senoh and T. Mukai, Jpn. J. appl. Phys. 30, L1708 (1991)

[11]Y. T. Rebane, Y. G. Shreter and W. N. Wang, Applied Surface Science 166, 300 (2000)

[12] S. Tomiya, T. Hino, S. Goto, M. Takeya and M. Ikeda, IEEE J. Sel. Top.

Quant. 10, 6, 1277 (2004)

[13] T. Detchprohm, K. Hiramatsu, H. Amano and I. Akasaki, Appl. Phys. Lett. 61, 2688 (1992),

[14] T. Kachi, K. Tomita, K. Itoh and H. Tadano, Appl. Phys. Lett. 72, 704 (1998)

[15] W. utsumi, H. Saitoh, H. Kaneko, T. Watanuki, K. Aoki and I. Shimomura, Nature Materials, 2, 735 (2003)

[16] E.T. Yu and M.O. Manaseh, "OPTOELECTRONIC PROPERTIES OF SEMICONDUCTORS AND SUPERLATICES, vol. 16, III-V Nitride Semiconductors: Applications and devices", 161, (2003) TAYLOR AND FRANCLS BOOKS, INC.

[17] P. Waltereit, O. Brandt, A. Trampert, H.T. Grahn, J.Menniger, > Ramsteiner, M. Reiche and K.H. Ploog, Nature Materials, 406, 865 (2000)

[18] S. Porowski, Mater. Sci. And Engineering, B44, 407 (1997)

[19] H. Yamane, M. Shimada, T. Sekiguchi and F.J. Disalvo, J. Crystal Growth, 186, 8 (1998)

[20] M. Aoki, H. Yamane, M. Shimada, S. Sarayama, H. Iwata and F.J. Disalvo, J. Crystal Growth, 266, 461 (2004)

[21] F. Kawamura, M. Morishita, K. Omae, M. Yoshimura, Y. Mori and T. Sasaki, Jpn. J. Appl. Phys. 42, L879 (2003)

[22] M. Morishitia, F. Kawamura, M. Kawahara, M. Yoshimura, Y. Mori and T. Sasaki, J. Crystal Growth, 270, 402 (2004)

[23] R. Dwilinski, R. Doradzinski, J. Garcznski, L. Sierzputowski, M. Paczewska,

A. Wysmolek and Kaminska, MRS Internet J. Nitride Semicond. Res. 3, 25 (1998)

[24] B. Wang, M.J. Callaha, K.D. Rakes, L.O. Bouthillette, S.Q. Wang, D.F. Bliss and J.W. Kolis, J. Crystal Growth, 287, 376 (2006)

[25] T. Hashimoto, F. Wu, J.S. Speck and S. Nakamura, Nature mater., 6, 568 (2007)

[26] C. R. Miskys, M. K. Kelly, O. Ambacher, and M. Stutzmann, Phys. Status Solidi C 0 1627 (2003)

[27] S. Nakamura, M. Senoh, S. Nagahama, N. Iwasa, T. Yamada, T. Matsushita, H. Kiyoku, Y. Sugimoto, T. Kozaki, H. Umemoto, M. Sano, and K. Chocho, Appl. Phys. Lett. 73 832 (1998)

[28] Mater. Res. Soc. Symp. Proc. 37 61 (2002)

[29] S. Bohyama, H. Miyake, K. Hiramatsu, Y. Tsuchida and T. Maeda, Jpn. J. Appl. Phys. 44 L24 (2005)

[30] H. Goto, S. W. Lee, H. J. Lee, Hyo-Jong Lee, J. S. Ha, M. W. Cho, T. Yao, Pys. Status Solidi C 5 1659 (2008)

[31] Phys. Status Solidi C 6 S313 (2009)

[32] S. W. Lee, H. Goto, T. Minegishi , W. H. Lee , J. S. Ha, H. J. Lee, Hyo-jong Lee, S. H. Lee, T. Goto, T. Hanada, M. W. Cho, T. Yao, Phys. Stat. Sol. (c) 4 2617 (2007)

[33] F. Lipski, S.B. Thapa, J. Hertkorn, T. Wunderer, and S. Schwaiger et al., Phys. Stat. Sol. C 1-4 (2009)

[34] X. weng, S. Raghavan, J.D. Acord, A. Jain, E.C. Dickey and J.M. Redwing, J.

Crystal Growth 300 217 (2007)

[35] H.S. Kim, M.D. Dawson, and G.Y. Yeom, J. Korean Phys. Soc. 40, 567 (2002)

[36] P.R. Tavernier and D.R. Clarke, J. Appl. Phys. 89, 1527 (2001)

[37] H. Tsuchiya, K. Sunaba, M. Minami, T. Suemasu, and F. Hasegawa, Jpn. J. Appl. Phys., Part2 37, L568 (1998)

[38] Y. Oshima, T. Eri, M. Shibata, H. Sunakawa and A. Usui, Phys. Stat. Sol., (a) 194, 554 (2002)

[39] S. Bohyama, H. Miyake, K. Hiramatsu, Y. Tsuchida and T. Maeda, Jpn. J. Appl. Phys., 44, L24 (2005)

Chapter2. Experimental

2.1) Growth method

2.1.1) Hydride Vapor Phase Epitaxy (HVPE)

As an epitaxy process that works near thermodynamic equilibrium, it is of particular interest for applications such as selective area growth, overgrowth of buried structures, and planar growth. The opportunity this process offers to efficiently manufacture extremely thick and pure compound semiconductor structures means that it has been recently used primarily in the manufacture of GaN substrates or template.
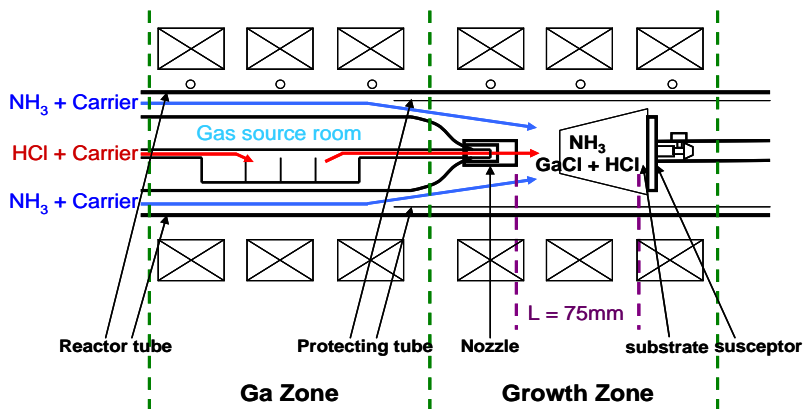
FIGURE 2.1 Schematic diagram of HVPE system

HVPE is a growth technique involving thermo-chemical reactions at

atmospheric pressure. The HCl and carrier gases flowing through the tubes, the materials inside the tube, and the temperature at the point of the reaction determine the reaction products. The final reaction leaves the desired material, which is deposited onto a substrate that is usually rotated at the end of the tube. The temperatures of the reactions and deposition can be independently controlled. Generally, the heating system is constituted of a multiple zone furnace. The possibility to separately set the partial pressure of each species, the chlorides and hydrides being independently produced, allows a systematic approach for searching the growth conditions.

HVPE system is consisted with a hot wall reactor made of quartz, which is located in a 6 zone furnace as shown in FIG. 2.1. The multi zone furnace was designed for the optimum control of source and substrate temperatures, and the delivery of all reactants. The HCl and H_2 carrier gases flowing through the tubes to Ga source room, the metallic Ga inside the tube. The temperature at the Ga source zone and GaN growth zone of the reaction were determined at 850^0C and 1040^0C, respectively as shown in FIG. 2.1.

The reaction of growth zone leaves the GaN material, which is deposited

onto a substrate that is rotated at the end of the tube. The epitaxial growth was

conducted at atmospheric pressure. The reactions in the reactor were as follow;

$$Ga(l) + HCl(g) \Rightarrow GaCl(g) + 1/2H_2(g)$$
$$GaCl(g) + NH_3(g) \Rightarrow GaN(s) + HCl(g) + H_2(g)$$
$$HCl(g) + NH_3(g) \Rightarrow NH_4Cl(l)$$
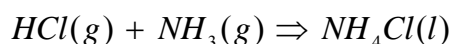
2.2) Characterization of measurement method

2.2.1) Scanning Electron Microscopy (SEM)

Scanning electron microscopy (SEM) has become one of the most versatile

and useful method for direct imaging, characterization, and studying of solid

surfaces. As the electrons penetrate the surface, a number of interactions occur that

can result in the emission of electrons or photons from (or through) the surface.

Appropriate detectors can collect a reasonable fraction of the electrons emitted,

and the output can be used to modulate the brightness of a cathode ray tube (CRT)

whose x- and y- inputs are driven in synchronism with the x-y voltages rastering

the electron beam. In the way an image is produced on the CRT. When the primary

electrons collide with atoms with atoms of a solid surface in the specimen the

electrons take part in various interactions.

The principle images produced in the SEM are of three types; secondary electron images, backscattering electron images, and elemental X-ray maps. Secondary and backscattering electrons are conventionally separated according to their energies. They are produced by different mechanisms.

When a high-energy primary electron interacts with an atom, it undergoes either inelastic scattering with atomic electrons or elastic scattering with the atomic nucleus. In an inelastic collision with an electron, some amount of energy is transferred to the other electron. If the energy transfer is very small, the emitted electron will probably not have enough energy to exit the surface. If the energy transferred exceeds the work function of the material, the emitted electron can exit the solid. When the energy of the emitted electron is less than about 50 eV, by convention it is referred to as a secondary electron (SE), or simply a secondary. Most of the emitted secondaries are produced much deeper in the material suffer additional inelastic collisions, which lower their energy and trap them in the interior of the solid.

Higher energy electrons are primary electrons that have been scattered without loss of kinetic energy (i.e., eleastically) by the nucleus of an atom,

although these collisions may occur after the primary electron has already lost some of its energy to inelastic scattering. Backscattered electrons (BSEs) are considered to be the electrons that exit the specimen with an energy greater then 50 eV, including Auger electrons.

However, most BSEs have energies comparable to the energy of the primary beam. The higher the atomic number of a material, the more likely it is that backscattering will occur. Thus a beam passes from a low-Z (atomic number) to a high-Z area, the signal due to backscattering, and consequently the image brightness, will increase. There is a built in contrast caused by elemental differences. It is usual to define the primary beam current i_0, the BSE current i_{BSE}, The SE current i_{SE}, and the sample current transmitted through the specimen to ground i_{SC}, such that the Kirchoff current law holds;

$$i_0 = i_{BSE} + i_{SE} + i_{SC}$$

These signals can be used to form complementary images. As the beam current is increased, each of these currents will also increase. The backscattered electron yield η and the secondary electron yield δ, which refer to the number of backscattered and secondary electrons emitted per incident electron, respectively,

are defined by the relationships.

$$\eta = \frac{i_{BSE}}{i_0}, \qquad\qquad \delta = \frac{i_{SE}}{i_0}$$

In most currently available SEMs, the energy of the primary electron beam can rage from a few hundred eV up to 30 keV. The Values of δ and η will change over this rage, however, yielding micrographs that may vary in appearance and information content as the energy of the primary beam is changed.[1]

2.2.2) High Resolution X-ray Diffraction (HRXRD)

2.2.21) Conventional high resolution X-ray

Conventional high resolution X-ray diffraction (HR-XRD) is a powerful tool for the non-destructive ex-situ investigation of epitaxial layers. The information which is obtained from diffraction patterns concerns the composition and uniformity of epitaxial layers, their thicknesses, the built-in strain and strain relaxation, and the crystalline perfection related to their dislocation density [2].

FIG. 2.2 shows the schematics of X-ray measurement system. It combines a four-crystal monochromator and a multiple-reflection analyzer crystal to perform high-resolution measurements for reciprocal lattice scans. A Ge (220) 4-crystal

monochromator added by the crossed slit attachment is used as an X-ray beam

source.
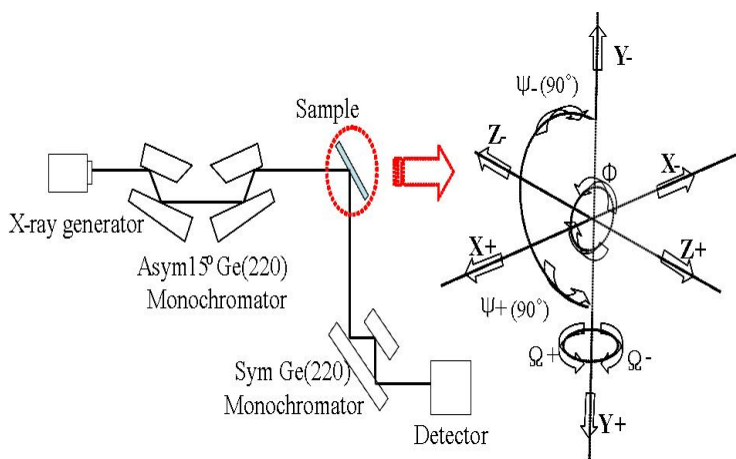
FIGURE 2.2 Schematic illustration of HRXRD geometry

The Ge 4-crystal monochromator produces a beam with very low divergence

and small wavelength spread. For example, approximate divergence of the Ge

(220) 4-crystal monochromator is 12 arcsec. The crossed slit collimator is designed

to provide a point x-ray source. The slit is variable in width up to 10 nm with a

step of 0.02 mm. The diffracted beam is detected by a double arm attachment

which is used for high resolution application. One arm is a rocking curve

attachment and the second arm carries the channel cut analyzer crystal to convert

to a triple axis mode. A Ge crystal with symmetric (220) reflection was used for

the analyzer. For the X-ray scans, a beam of parallel and monochromatic x-rays of wavelength λ is incident on a crystal at an angle θ_B, Bragg angle, which is measured between the direction of the incident beam and the crystal plane under consideration.

2.2.2.2) ω scan (rocking curve) and ω-2θ scan

Any measurement of lattice spacing is in principle determined by Bragg law. This equation follows from kinematic diffraction theory and neglects the fact the that the refractive index of matter for X-ray is less than 1 by a few parts in 10^{-6} and so the incident beam is refracted to an internal angle slightly smaller than the external one.

In FIG. 2.3, two possible scans for measuring the intensity of Bragg reflection due to the reciprocal lattice point (hkl) are indicated: (i) Conventional powder diffraction uses a ω-2θ scan for measuring symmetric Bragg reflections. For such a scan, the detector is rotated twice as fast and in the same direction around the diffractometer axis as the sample.

In reciprocal space (Figure 2.4), this conventional motion of sample and detector corresponds to a change of k_s in the following way: the tip of vector k_s moves along the reciprocal lattice vector G_{hkl}. During this motion the angle ω between the incident beam and the sample surface changes. For asymmetric (hkl) Bragg reflections, ω-2θ scan direction runs also radial from the origin (000) of the reciprocal space along G_{hkl} (FIG. 2.3a) (ii) In the ω-scan, the detector is fixed in position with wide open entrance slits and the sample is rotated, i.e. ω changes. In reciprocal space, this corresponds to a path as indicated in figure 2.8b by bold arrow. The scan direction is transversal in reciprocal pace. Thus the so-called rocking curve is obtained. In reciprocal space, this corresponds to a path as shown in FIG. 2.3. When i consider about rocking curve of heteroepilayers, there exist difference of diffraction angle between the layer and substrate, which is caused by tilt or mismatch. Double or mulitiple peaks will therefore arise in the rocking curve. Peaks may be broadened by defects if these give additional rotations to the crystal lattice, and there will also be small peaks arising from interference between waves scattered from the interfaces, which will be controlled by the layer thickness. The

material will show different defects in different regions. Table 2.1 summarizes the

influence on the rocking curve of the important parameter [3].

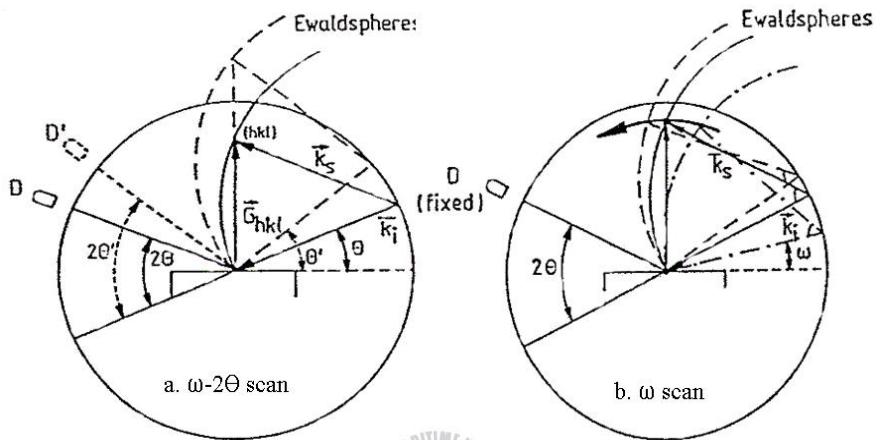**FIGURE 2.3 Ewald sphere construction (for symmetric reflections, i.e. reflecting planes are parallel to the surface) for the ω-2θ scan geometry. The bold arrow indicates the movement in the reciprocal lattice**
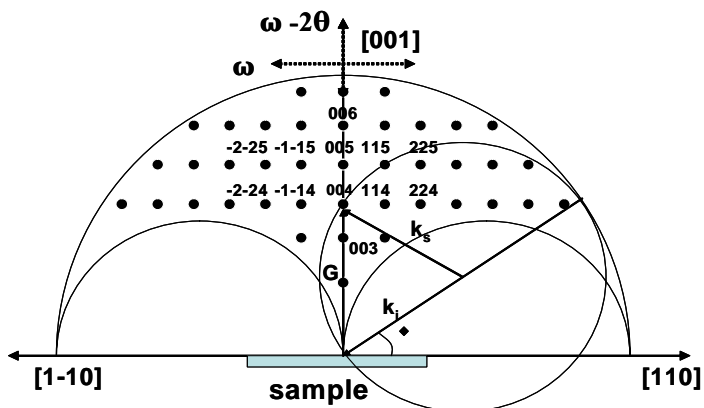
FIGURE 2.4 Reciprocal space map showing accessible range for Bragg reflection measurement.

TABLE 2.1 The effects of substrate and epilayer parameters upon the rocking curve.

Material parameter	Effect on rocking curve	Distinguishing features
Mismatch	Splitting of layer and substrate peak	Invariant with sample rotation
Misorientation	Splitting of layer and substrate peak	Changes sign with sample rotation
Dislocation content	Broadening peak	Broadening invariant with beam size No shift of peak with beam position on sample.
Mosaic spread	Broadening peak	Broadening may increase with beam size, up to mosaic cell size
Curvature	Broadening peak	Broadening increases linearly with beam size, Peak shifts systematically with beam position on sample
Relaxation	Changes splitting	Different effect on symmetrical and asymmetrical reflection
Thickness	Affects intensity of Peak	Integrated intensity increases with layer thickness, up to a limit
Inhomogeneity	Effects vary with position on sample	Individual characteristics may be mapped

2.2.3) Photoluminescence (PL)

Photoluminescence is one of the characterization methods to evaluate the optical properties of compound semiconductors. PL is a nondestructive method that gives various information about both intrinsic and radiative recombination processes associated with imperfections of a crystal induced by impurities or

dislocations.

The schematic diagram of PL measurement system is shown in Fig. 2.5. As an optical excitation light source, He-Cd laser with wavelength of 325nm was used and samples were fixed in a cryostat capable of varying temperature from 10K to room temperature(RT). Excited light was dispersed by a 32 cm monochromator with 1200 g/mm grating and detected by a charge coupled device (CCD) camera.
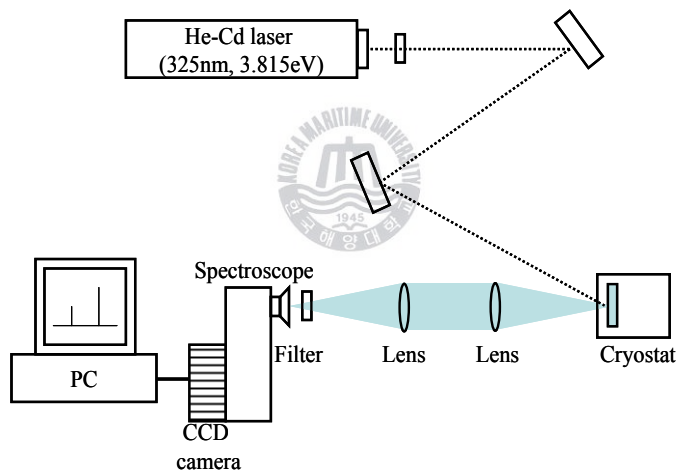
FIGURE 2.5 Experimental setup of the PL measurement system used in this study.

As electron-hole pairs (EHP) in excess of their equilibrium number are created in the crystals by the incident laser source, they settle in states near the minimum of the conduction band (E_c) in case of electrons and maximum of Valence band (E_v) in case of hole, respectively. These electrons and holes (carriers)

are considered to be in quasi-thermal equilibrium states and decay by recombination via several kinds of transitions showed in FIG. 2.6. E_g means the band-gap of a semiconductor and incident light should have higher energy than this to excite carrier up to conduction band; GaN has approximate 3.39 eV of band-gap at room temperature (RT, ~300K).

Generally, photoluminescence by (b) is called free-exciton transition and this is dominantly observed peak at RT. (c) and (d) are transitions by exciton bound to neutral acceptor and donor, and (e) and (f) are transitions of (d) and (c) induced by ionized impurities, respectively. Finally, (g) is a transition from a donor to an acceptor level.
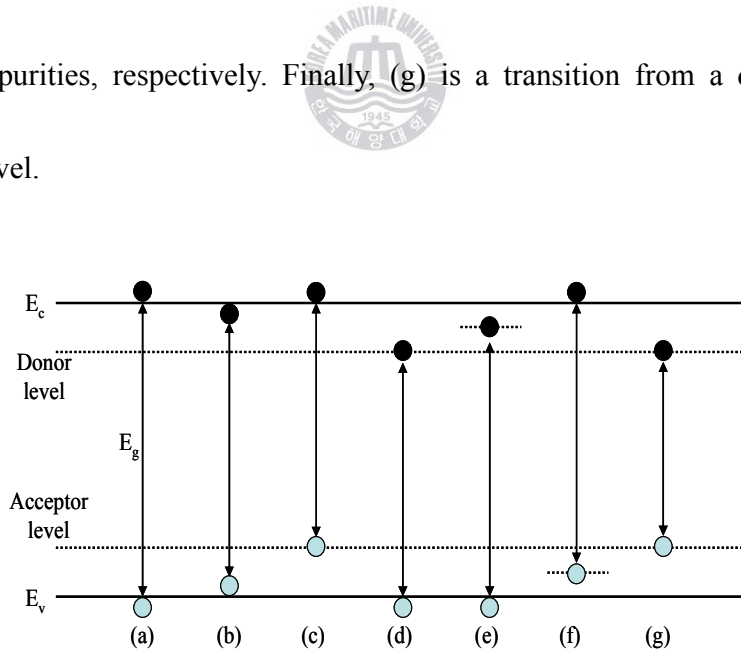
FIGURE 2.6 Radiative recombination processes in a semiconductor. Every transition accompanies an emission of energy as a light with different wavelength.

Above this, standard transitions are simply explained. However, there exists more complex kind of peaks in real measurement of PL, due to phonons or impurities. The myriad of optical transitions that could be and have been observed in the luminescence spectra of GaN associated with defects was summarized as shown in TABLE 2.2 [4]

The list shows a schematic description of the related transitions and energy positions within the gap of the defect. TABLE 2.2 tabulates their nomenclature and provides brief comments. The energy position of the luminescence lines and bands may depend on strain in thin GaN layers, temperature, and excitation intensity.

Therefore, in TABLE 2.2 the energy positions corresponding to the strain-free GaN at low temperature are given.

TABLE 2.2 List of main luminescence lines and bands in GaN [4]

Maximum position (eV)	Nomeclature	Doping	Comments
3.478	FX_A, FE, X_A	Undoped	
3.471	D^oX, DBE, D^oX_A	Undoped, Si	A few close lines
3.466	A^oX, ABE, A^oX_A	Undoped, Mg	Best FWHM < 0.1meV
3.44-3.46	TES	Undoped	Plethora of lines
3.455	ABE	Zn	A weaker peak at 3.39eV
3.45-3.46	Y_1	Undoped	Correlates with inversion domains
3.41-3.42	Y_2	Undoped	
3.397		Be	e-A type
3.387	FX_A-1LO, FE-LO	Undoped	
3.38	DBE-LO	Undoped	
3.38		Be	DAP type
3.37-3.38	Y_3	Undoped	
3.375	ABE-LO	Undoped	
3.364	ABE-LO	Zn	
3.35-3.36	Y_4	Undoped	
3.34	Y_5	Undoped	
3.30-3.32	Y_6	Undoped	
3.295	FX_A-2LO, FE-2LO	Undoped	
3.288	DBE-2LO	Undoped	
3.283	ABE-2LO	Undoped	
3.28	UVL	Undoped	e-A type
3.272	ABE-2LO	Zn	
3.27	DBE	DBE in cubic GaN	
3.26	UVL	Undoped, Si	DAP type
3.1-3.26	UVL	Mg	e-A and DAP
3.21-3.23	Y_7	Undoped	
3.16			Shallow DAP in cubic GaN
3.08	Y_8	Undoped	
3.0-3.05	BL	C	Broad

49

Reference

[1] Guozhong Cao, Nanostructures & Nanomaterials, Imperial College Press (2004)

[2] Günther Bauer, Wolfgang Richter, "Optical Characterization of Epitaxial Semiconductor Layers" 1st edition (Springer-Verlag Berlin heidelberg, 1996), p287

[3] D.K. Bowen and B.K. Tanner: " High resolution X-ray Diffraction and Topography" (Taylor & Francis Ltd, London, United Kingdom, 1998), p52

[4] Michael A. Reschikov and Hadis Morkoc, J. Appl. Phys. 97, 061301 (2005)

Chapter3. Comparison of GaN on Zn-polar/O-polar ZnO

3.1) Introduction

Although freestanding (FS)-GaN substrates grown by hydride vapor phase epitaxy (HVPE) have been commercialized. Application of FS-GaN to the fabrication of device such as light emitting diodes and laser diodes are progressing slowly. This is mainly because FS-GaN substrates are expensive owing to the difficulty of manufacturing process. Removing of thick GaN layers from the sapphire substrates are difficult because sapphire substrates are robust material with a negligible etching rate for any etchant. For this reason, various attempts such as laser lift-off [1-2], mechanical substrate polishing [3], void-assisted separation (VAS) [4], and facet controlled epitaxial lateral overgrowth (FACLEO) [5] have been developed to remove sapphire substrate [1,6]. However, the laser lift-off technique has a fracturing problem during laser irradiation [7]. While the other approaches require complex processes such as deposition of mask materials and growth of GaN template prior to growth of the thick-GaN by HVPE. Therefore, recently new approaches are developed like as self-separation of evaporable buffer

layer (EBL) [6], and chemical lift-off (Metal-Nitride) [5], but those method

requests to surmount several problems comes from the narrow growth window of

amorphous (NH$_4$Cl) layer and different crystal structure of metal-nitride template

[5-6]. Therefore, more simple and easy way for the growth and separation of GaN

crystal is important especially for the practical point of view.

A simple self-separation technique by using a sacrificial interlayer made of

ZnO have proposed that can be easily etched without protecting cover layer in the

HVPE process. Because of its similar material properties compared to GaN, ZnO

is an ideal candidate for that purpose. Same crystal structure and especially the

small lattice mismatch of only about 1.8 % (c-axis) and 0.4% (a-axis), the fact that

ZnO can be easily etched makes it very attractive. However the extreme instability

of ZnO in the HVPE atmosphere demands a protecting cover layer of GaN before

growth [7-8].

First of all, the effect of ZnO polarity for GaN on ZnO growth will be

described based on the chemical stability of ZnO polarity, surface morphology and

crystalline.

3.2) Experimental details

250nm thick single crystal ZnO layer grown on c-plane sapphire was prepared by plasma assisted molecular beam Epitaxy (PA-MBE). The polarity of ZnO is controlled by using a MgO buffer. Polarity controlled ZnO was grown on c-sapphire substrate for HVPE film GaN growth by PA-MBE [9]. GaN films about 4 μm were grown on Zn-/O-polar ZnO templates with one-step growth method based on HVPE. In HVPE growth, HCl gas was reacted with metallic Ga to form GaCl, and then the GaCl gas was transferred into the growth region to react with NH_3. I used N_2 as a carrier gas in order to protect ZnO from etching in HVPE growth atmosphere. According to GaN on Zn-polar ZnO and O-polar ZnO were compared to the characteristics of GaN layers after growth.

3.3) ZnO etching rate of GaN after growth

FIG. 3.1 shows a ZnO etching rate of sample-A; (Zn-polar ZnO) and Sample-B; (O-polar ZnO template) after GaN growth at the same growth conditions. Sample-A and sample-B show respective ZnO etching rates about 50nm and 180nm during the GaN growth. The etching rate of sample-B is about

4times higher than the Sample-A. That reveal higher chemical stability of sample-A than sample-B.
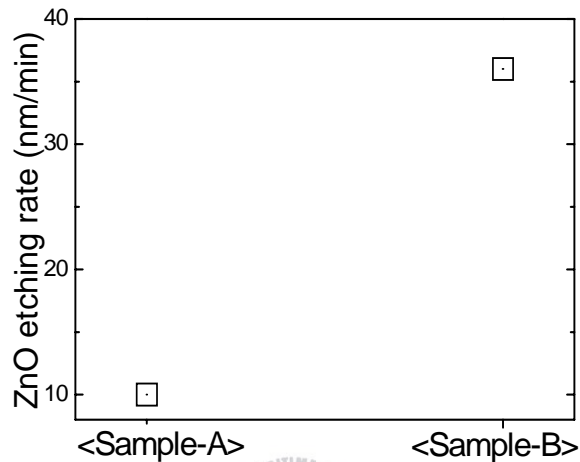
FIGURE 3.1 ZnO etching rate of GaN after growth of sample-A(GaN/Zn-polar ZnO/c-Al$_2$O$_3$) and sample-B(GaN/O-polar ZnO/c-Al$_2$O$_3$)

3.4) Surface morphology and PL Intensity

FIG..3.2 shows the PL spectra measured at room temperature for sample-A and sample-B. Sample-A has 2.15 times higher emission intensity than the sample-B. And a clear signal from the GaN at 3.44 eV could be detected from the PL spectrum, as well as a peak related to ZnO at 3.34eV. The broad luminescence band at around 2.9eV is typical for Zn doped GaN [10], probably a result of gas phase diffusion during growth. [8]

The inset of Figure 2 shows a plan view SEM images of sample-A and sample-B Sample-A shows relatively smoother surface morphology than Sample-B.
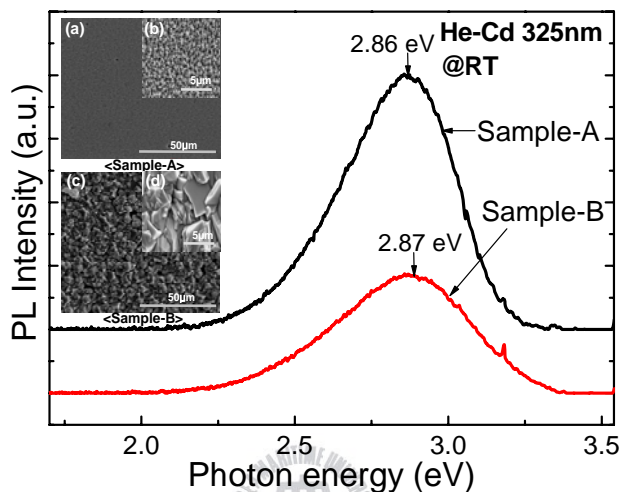
FIGURE 3.2 RT measurements of sample-A(GaN/Zn-polar ZnO/c-Al₂O₃) and sample-B(GaN/O-polar ZnO/c-Al₂O₃) and inset plane view SEM images of sample-A and sample-B indicated (a)-(b) and (c)-(d) each other 50µm and 5µm and 50µm and 5µm.

3.5) Conclusion

The effect of Zn-/O-polar ZnO on chemical and crystallinity of GaN layers has been investigated. Zn-polar ZnO revealed the chemical stability, smooth surface morphology and buffer crystallinity than O-polar ZnO after GaN growth. So based on these results, I decided to grow GaN on Zn-polar ZnO template for the application of freestanding GaN substrate.

Reference

[1] C. R. Miskys, M. K. Kelly, O. Ambacher, and M. Stutzmann, Phys. Status Solidi C 0 (2003) 1627

[2] S. Nakamura, M. Senoh, S. Nagahama, N. Iwasa, T. Yamada, T. Matsushita, H. Kiyoku, Y. Sugimoto, T. Kozaki, H. Umemoto, M. Sano, and K. Chocho, Appl. Phys. Lett. 73 (1998) 832

[3] Mater. Res. Soc. Symp. Proc. 37 (2002) 61

[4] S. Bohyama, H. Miyake, K. Hiramatsu, Y. Tsuchida and T. Maeda, Jpn. J. Appl. Phys. 44 (2005) L24

[5] H. Goto, S. W. Lee, H. J. Lee, Hyo-Jong Lee, J. S. Ha, M. W. Cho, T. Yao, Pys. Status Solidi C 5 (2008) 1659

[6]Phys. Status Solidi C 6 (2009) S313

[7] S. W. Lee, H. Goto, T. Minegishi, W. H. Lee, J. S. Ha, H. J. Lee, Hyo-jong Lee, S. H. Lee, T. Goto, T. Hanada, M. W. Cho, T. Yao, Phys. Stat. Sol. (c) 4 (2007) 2617

[8] F. Lipski, S.B. Thapa, J. Hertkorn, T. Wunderer, and S. Schwaiger et al., Phys. Stat. Sol. C 1-4 (2009)

[9] T. Minegishi, T. Suzuki, C. Harada, T. Goto, M. W. Cho and T. Yao, Curr. Appl. Phys. 4, (2004) 685

[10] H. Teisseyre, P. Perlin, T. Suski, I. Grzegory, J. Jun and S. Porowski, J. Phys. Chem. Solids 56, (1995) 353

Chapter4. Optimization of growth condition for high quality GaN grown on ZnO template

4.1) Introduction

FS-GaN substrates are expensive owing to the difficulty of manufacturing process. Hence, more simple and easy way for the growth and separation of GaN thick film is crucial for the practical point of view. A simple self-separation technique was proposed by using a sacrificial interlayer made of ZnO without protecting cover layer in the HVPE process [1-2].

This requires special growth sequences for the fabrication of FS-GaN. So, I have optimized the growth condition. The growth condition of GaN on Zn-polar ZnO template layers will be mentioned in this chapter. I have investigated and will explain on the effect of growth temperature and V/III flow ratio in chapter 4.

4.2) Experimental details

My prepared 250nm thick single crystal ZnO layer as described in the section 3.2). GaN films about 4μm were grown Zn-polar ZnO template on

substrate with one-step growth method based on HVPE. In HVPE growth, HCl gas was reacted with metallic Ga to form GaCl, and then the GaCl gas was transferred into the growth region to react with NH_3. I used N_2 as a carrier gas in order to protect ZnO from etching of growth condition optimized growth temperature to 750^0C from 1050^0C and change of flow rate of $V(NH_3)/III(HCl)$ ratio to 10 from 80 then identified with growth conditions.

4.3) Effect of the growth temperature for GaN on ZnO growth

4.3.1) ZnO etching rate after GaN growth

Growth conditions was optimized for the direct growth of GaN on ZnO template. Because, ZnO can be easily etched by growth temperature and HCl and NH_3 which are commonly used in the HVPE growth of GaN.[3] First of all, I optimized the growth temperature for GaN grown on Zn-polar ZnO template.

TABLE 4.1 shows the growth temperature (a)-(d) from 1050 ^0C to 750 ^0C, ZnO etching rate and GaN growth rate. As the growth temperature increasing, ZnO etching rate increased too. The ZnO etching rate is expected about more than 36.16nm/min in the 1050^0C. Because the prepared ZnO template was almost

eliminated so exact etching rate was not evaluated. GaN growth rate was increased

by increasing the Ga source supplying. However GaN growth rate between (b) and

(c) looks like similar. Because, the partial pressure of GaCl is almost similar over

than $800\,^0$C [4].

TABLE 4.1 Growth temperature dependence on
ZnO etching rate and GaN growth rate

T_g (growth temperature)	ZnO etching rate (nm/min)	GaN growth rate (nm/min)
(a) 750 ^{0}C	6.03	440.96
(b) 850 ^{0}C	10.23	762.57
(c) 950 ^{0}C	18.91	780.25
(d) 1050 ^{0}C	36.16	

4.3.2) Surface morphology

FIG. 4.1 shows the surface morphology of samples. Generally, GaN growth

temperature is over the 1000 ^{0}C in HVPE method [5]. Nevertheless, in this study,

GaN film was grown below 1000 ^{0}C for the direct growth of GaN on ZnO FIG. 4.1

(a) and (b) show similar morphology. But FIG. 4.1 (c) shows rough surface with

many pits. Eventually, FIG. 4.1 (d) GaN growth was not achieved due to high

vapor pressure of ZnO. This result indicates that the growth of GaN on ZnO is

possible in low temperature range from 750 ^{0}C to 850 ^{0}C.

The effects of growth temperature on the crystallinity of a 4μm thick GaN films were investigated by high resolution X-ray diffraction (HRXRD). The full width at half maximum values (FWHM) of (0002) X-ray ω-rocking curves were measured for the evaluation of structural quality of GaN layers.
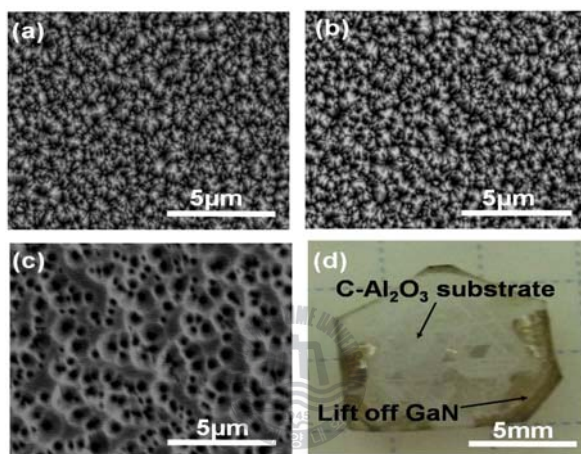

FIGURE 4.1 SEM images of GaN grown on Zn-polar ZnO with various GaN growth temperature and growth temperature of GaN was (a) 750⁰C, (b) 850⁰C, (c) 950⁰C and (d) 1050⁰C respectively.

4.3.3) Evaluation of structural property by HRXRD

FIG. 4.2 (a) shows that the FWHM of (0002) X-ray ω-rocking curves (XRC). The crystallinity of GaN film was poor at $750^{\circ}C$. but improved at the growth temperature of $850\ ^{0}C$ or $950\ ^{0}C$. The FWHM values are less than those of ZnO template layer. And FIG. 4.2 (b) shows that similar growth rate for $850\ ^{0}C$ and

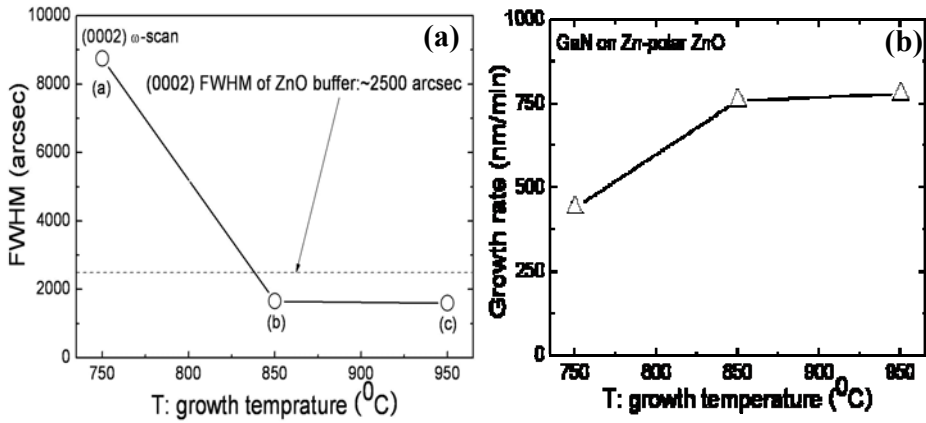950 ^{0}C. Because GaCl has similar partial pressure from 800 ^{0}C to 1000 ^{0}C.[3]

FIGURE 4.2 XRD measurement results for the omega scans on the GaN.
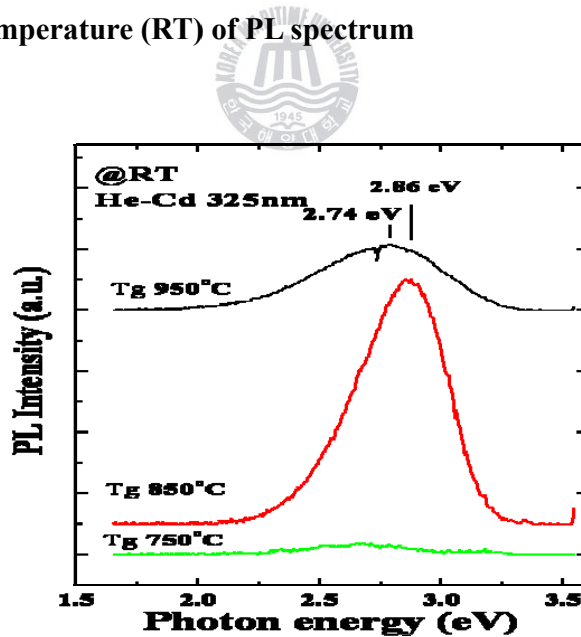
4.3.4) Room temperature (RT) of PL spectrum

FIGURE 4.3 PL measurement results at room temperature (RT)

FIG. 4.3 shows the PL spectra measured at room temperature. GaN grown at

850°C shows the strongest PL intensity at around 2.9 eV. The broad luminescence band at around 2.9eV was observed for Zn doped GaN [6], because of gas phase diffusion during growth. [7]

4.4) Effect of the V/III ratio for GaN on ZnO growth

4.4.1) ZnO etching rate after GaN growth

The V/III ratio was optimized. Source supplying was carefully controlled to be reached simultaneously on a Zn-polar ZnO template surface. The V/III ratio is defined as a flow rate of $V(NH_3)/III(HCl)$.

TABLE 4.2 $V(NH_3)/III(HCl)$ ratio and ZnO etching rate and GaN growth rate

V/III ratio (NH_3 / HCl)	ZnO etching rate (nm/min)	GaN growth rate (nm/min)
(a) 10	10.05	680.69
(b) 30	9.02	1002.01
(c) 50	9.61	760.59
(d) 80	10.52	640.74

TABLE 4.2 shows V/III ratio ZnO etching rate and GaN growth rate. As V/III ratio increasing, negligible change of ZnO etching rate was observed. The GaN growth rate is not strongly depend on the V/III ratio. Also, the GaN growth

rate is strongly depend on the V/III ratio. But, the GaN growth rate is affected by the pressure of reactor.(the difference in atmospheric pressure due to weather change; 30mTorr)

4.4.2) Surface morphology

FIG. 4.4 shows surface morphology of GaN after growth by using cross-sectional SEM images.
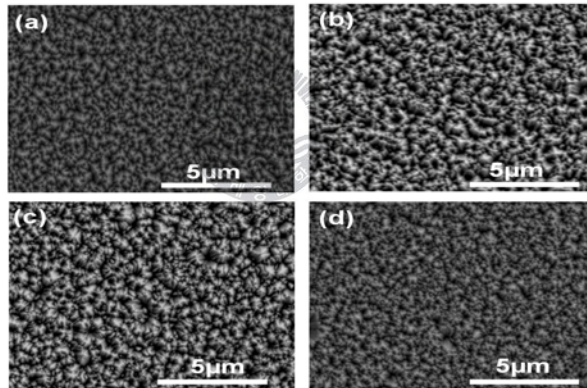

FIGURE 4.4 SEM images of GaN grown on Zn-polar ZnO with various flow V(NH₃)/III(HCl) ratio. The flow ratio was (a) 10, (b) 30, (c) 50 and (d) 80, respectively.

It is clear that the surface morphology and ZnO etching rate are independent on V/III ratio. The effects of V/III ratio on the crystallinity of GaN films were investigated by high resolution X-ray diffraction (HRXRD). The full width at half

maximum values (FWHM) of (0002) X-ray ω-rocking curves were measured for

the evaluation of GaN layers as with the effects of growth temperature study.

4.4.3) Evaluation by HRXRD

FIG. 4.5(a) shows that the FWHM variation of (0002) X-ray ω-rocking

curves (XRC) along with V/III ratio.
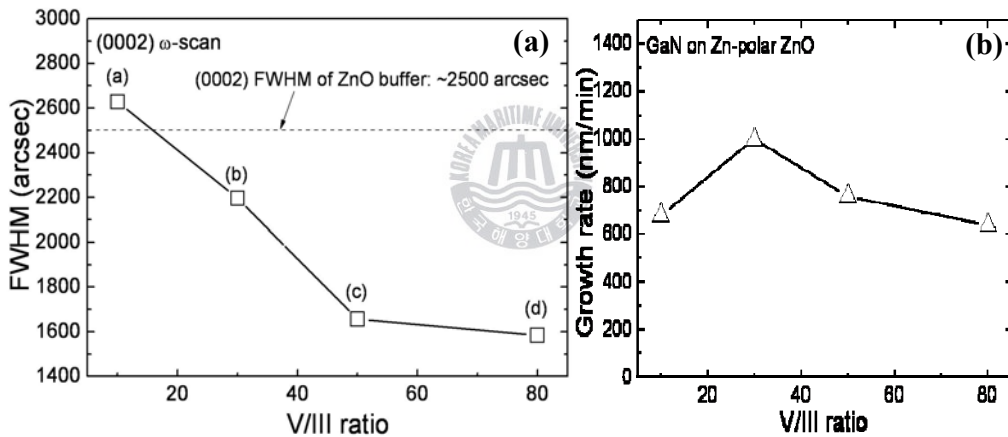

FIGURE 4.5 XRD measurement results for the omega scans on the GaN.

When the V/III ratio is larger than 10, the FWHM values of GaN is narrower

than the ZnO template layer, when the V/III ratio is 50 and 80, XRC FWHM was

considerably narrower than that of ZnO. FIG 4.5(b) shows that Growth rate is not

strongly depend on V/III ratio. Because the GaN growth rate was similar for all

samples, the crystal quality of GaN was attributed to the V/III ratio change.

4.4.4) Room temperature (RT) of PL spectrum

FIG. 4.6 shows the PL spectra measured at room temperature. Luminescence

band at around 2.9 eV dominate the spectrum. Higher V/III ratio is preferred in

terms of PL intensity. The broad luminescence band at around 2.9eV is assigned to

an acceptor bound exciton (Zn doped GaN) [6] Based on the morphology, XRC,

and PL results, I determined optimum V/III ratio as 50 for HVPE GaN on Zn-polar

ZnO template.

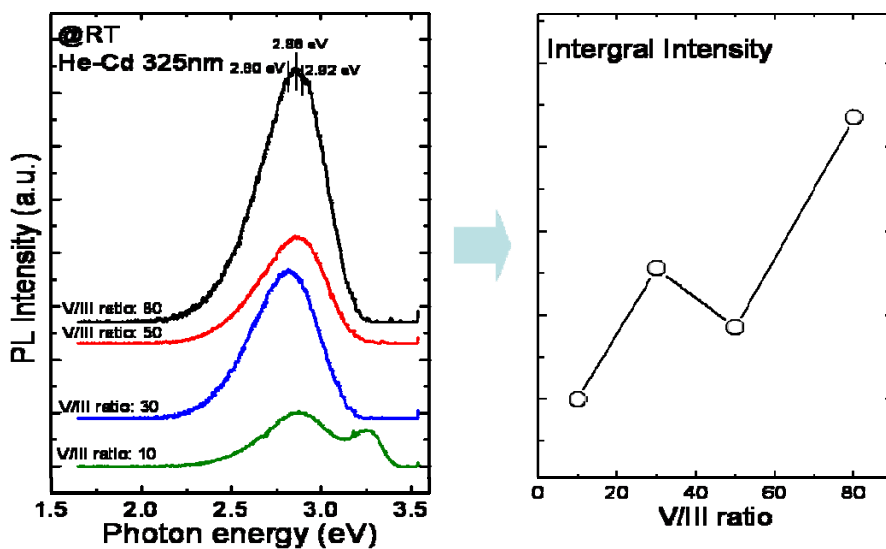**FIGURE 4.6 PL measurement results for room temperature (RT)**

4.5) Conclusion

The effects of growth temperature and V/III flow ratio on surface morphology and chemical stability and crystallinity of subsequently grow GaN films by HVPE have investigated. As a result growth temperature of 850^0C and the V/III ratio of 50 are determined as the optimum growth condition for the direct growth of GaN on ZnO template.

Reference

[1] S. W. Lee, H. Goto, T. Minegishi , W. H. Lee , J. S. Ha, H. J. Lee, Hyo-jong Lee, S. H. Lee, T. Goto, T. Hanada, M. W. Cho, T. Yao, Phys. Stat. Sol. (c) 4 (2007) 2617

[2] F. Lipski, S.B. Thapa, J. Hertkorn, T. Wunderer, and S. Schwaiger et al., Phys. Stat. Sol. C 1-4 (2009)

[3] A. Koukitu, S. I. Hama, T. Taki and H. Seki, Jpn. J. Appl. Phys. 37 (1998) 762

[4]Phys. Stat. Sol. (a) 194, No.2, 528-531 (2008)

[5] S. Gu, R. Zhang, Y. Shi, Y. Zheng, L. Zhang and T.F. Kuech, Appl. Phys. A 74 (2002) 537

[6] H. Teisseyre, P. Perlin, T. Suski, I. Grzegory, J. Jun and S. Porowski, J. Phys. Chem. Solids 56, (1995) 353

[7] F. Lipski, S.B. Thapa, J. Hertkorn, T. Wunderer, and S. Schwaiger et al., Phys. Stat. Sol. C 1-4 (2009)

Chapter5. Fabrication of Freestanding GaN substrate

5.1) Introduction

Although there are many approaches to obtain the free-standing GaN (FS-GaN) substrate by HVPE method, removing processes of the sapphire substrate from a thick GaN film is normally difficult so, self-separation technique is the most promising method for the fabrication of GaN substrate because it can make GaN substrate with more laser size and high quality.

By such reasons, void assisted self-separation (VAS) [1] and facet-controlled epitaxial lateral overgrowth (FACELO) [2] technique have been developed. But, these techniques need some complex processes such as Ti [1] or SiO_2 [2] deposition on MOCVD GaN template, prior to the thick GaN growth by HVPE. Therefore, recently new approaches are developed like as self-separation of evaporable buffer layer (EBL) [3], and chemical lift-off (Metal-Nitride) [2], but those method requests to surmount several problems comes from the narrow growth window of amorphous (NH_4Cl) layer and different crystal structure of metal-nitride template [2-3]. Therefore, self-separation technique by using ZnO

chemical etching is simpler than VAS and other lift-off methods.

In this chapter, I will discuss about the self-separation and fabrication of thick GaN which was directly grown on ZnO template.

5.2) Experimental details

In the chapter 3 and 4, I described on the direct growth of GaN on ZnO template. The ZnO layer was removed in The HVPE reactor, NH_4 gas atmosphere (850^0C to 1 minute) was conducted by etching. And then the H_2 gas atmosphere (900^0C to 1 minute) was conducted by etching. And finally, H_2 gas atmosphere ($1000\ ^0C$ to 1 minute) was conducted to remove the ZnO template. By this process removes the ZnO sacrificial layer. Consequently, 4μm-thick Freestanding GaN film was obtained. And, GaN layer was re-grown under the GaN growth condition (T_G: 1050^0C, V / III ratio ~ 50).[4] And, the property re-grown Freestanding GaN substrate was compared.

5.3) Fabrication sequence of the self-separated FS-GaN substrate

FIG. 5.1 shows the production process for FS-GaN. First of all, FIG. 5.1(a);

the growth condition of GaN film grown on Zn-ZnO template was confirmed. GaN

film grown on Zn-polar ZnO template was prepared. FIG 5.1(b); ZnO was

removed by chemical 3-step gas phase etching. (Step1: NH_4 gas atmosphere at

850^0C for 1minute, Step2: H_2 gas atmosphere at 900^0C for 1minute, Step3: H_2 gas

atmosphere at $1000\ ^0C$ for 1 minute). Re-growth of Freestanding GaN was

conducted under the (Growth temperature of 1050^0C, and V / III ratio of ~ 50.[4]

For sample-(a), 80 μm-thick GaN was re-grown, and for sample-(b), 400 μm-thick

GaN was re-grown on the GaN template. Bending was observed from the sample-

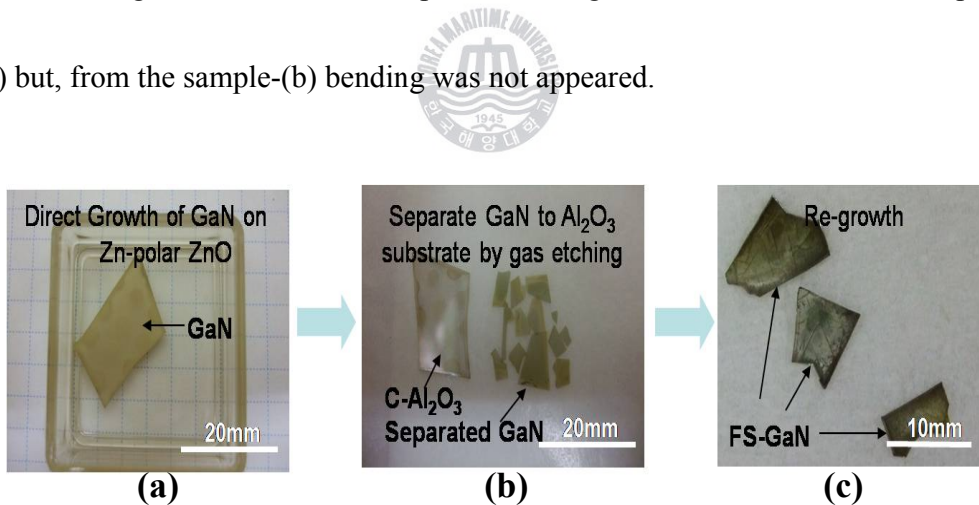(a) but, from the sample-(b) bending was not appeared.

FIGURE 5.1 Fabrication sequence of the Self-separated FS-GaN substrate by chemical etching.

5.4) Evaluation by HRXRD

FIG. 5.2 shows that X-ray rocking curve of FS-GaN (0002). Sample-(a) and

Sample-(b) show narrow FWHM of 936 arcsec and 972 arcsec, respectively. Although, the thickness is differ, FWHM values of two samples are similar to each other.
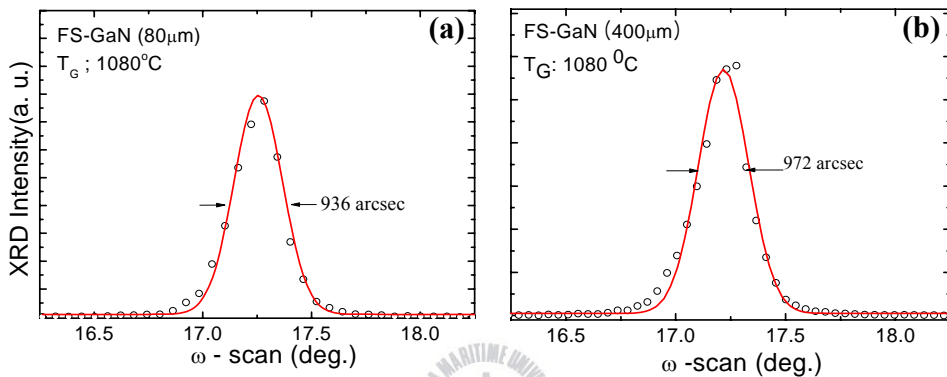

FIGURE 5.2 X-ray rocking curve of Freestanding GaN with the thickness of (a) 80μm and (b) 400μm

5.5) Low temperature Photoluminescence (PL) properties

The low-temperature (12K) PL spectra taken from the top-surface of the final free standing samples as shown in FIG. 5.3. Sample-(b) shows less intensity at the 2.9 eV and the UV peak at 3.364 eV dominate the spectrum indicating higher optical quality of sample-(b).
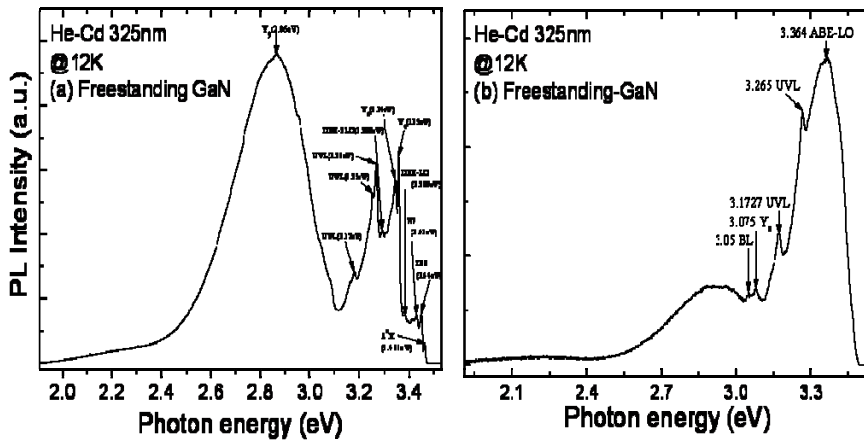
FIGURE 5.3 PL measurement results for Low-temperature (LT) 12K in the Freestanding GaN of thickness at (a) 80μm and (b) 400μm

5.6) Temperature dependence Photoluminescence (PL) properties

FIG. 5.4 shows temperature dependant of PL spectra of sample (a) and sample-(b). The PL spectra were measured in the temperature range of 15K to 300K. Sample-(a) shows strong deep level emission at low temperature, but it disappeared above 250K. But, deep level intensity was less intense than sample-(b), also it disappeared from 80K.
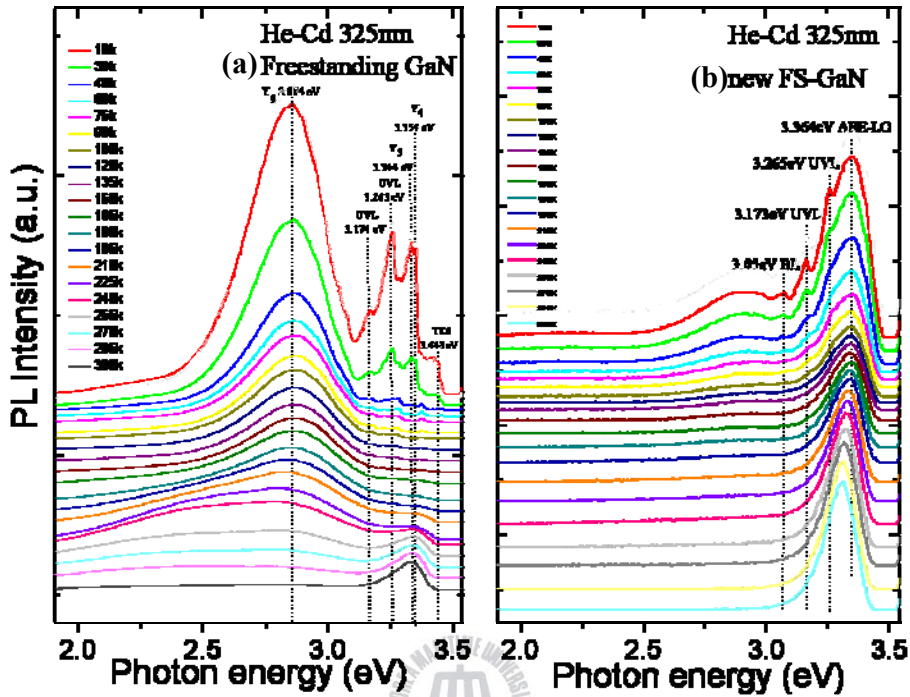
FIGURE 5.4 Temperature dependent PL measurement
results for (a) 80μm and (b) 400μm

5.7) Conclusion

A new technique of fabricating free-standing GaN substrate by direct growth

on ZnO template has been developed. The free-standing GaN film grown on Zn-

polar ZnO template is demonstrated by HVPE without an assistance of GaN

protecting cover layer.

Reference

[1] S. Bohyama, H. Miyake, K. Hiramatsu, Y. Tsuchida and T. Maeda, Jpn. J. Appl. Phys. 44 (2005) L24

[2] H. Goto, S. W. Lee, H. J. Lee, Hyo-Jong Lee, J. S. Ha, M. W. Cho, T. Yao, Pys. Status Solidi C 5 (2008) 1659

[3]Phys. Status Solidi C 6 (2009) S313

[4] S. W. Lee, H. Goto, T. Minegishi, W. H. Lee, J. S. Ha, H. J. Lee, Hyo-jong Lee, S. H. Lee, T. Goto, T. Hanada, M. W. Cho, T. Yao, Phys. Stat. Sol. (c) 4 (2007) 2617

[5] T. Minegishi, T. Suzuki, C. Harada, T. Goto, M. W. Cho and T. Yao, Curr. Appl. Phys. 4, (2004) 685

Chapter6. Summary and conclusion

This thesis will contribute to solve the critical problems of fabrication of FS-substrate, complexity of fabrication process and difficulty in fabrication of GaN substrate. This thesis has introduced ZnO sacrificial layer to fabricate FS-GaN and has demonstrated the growth of high quality FS-GaN. ***In the chapter 3***, The effect of Zn-/O-polar ZnO on chemical and crystalline properties of GaN grown GaN layers has been investigated. Zn-polar ZnO is apt to grow high quality GaN in terms of chemical-stability, smooth surface morphology and better crystallinity of overgrown GaN. ***In the chapter 4***, The effects of growth temperature and V/III ratio on the surface morphology, chemical stability and crystallinity of subsequently grown GaN films have been studied. Optimum growth condition for GaN on ZnO formation; growth temperature of 850^0C and V/III ratio of 50 has been determined. ***In the chapter 5,*** A new self-separation method by using ZnO template, directly grown GaN in HVPE and chemical etching has been developed. I succeed to obtain freestanding GaN film by HVPE without an assistance of GaN protecting cover layer.

As a result, self-separation technique by ZnO template layer for the fabrication of FS-GaN substrates has been developed. The thick GaN film grown on the ZnO template layer was separated from the c-sapphire substrate by gas phase chemical etching. This thesis proved that direct growth of GaN on ZnO template is useful to fabricate next-generation FS-GaN substrate and devices.

Appendix A

A-1. Physical properties of ZnO

Features of ZnO

- Wurtzite structure

- UV-bandgap→ UV applications

- Non-toxicity → cosmetics, medicine
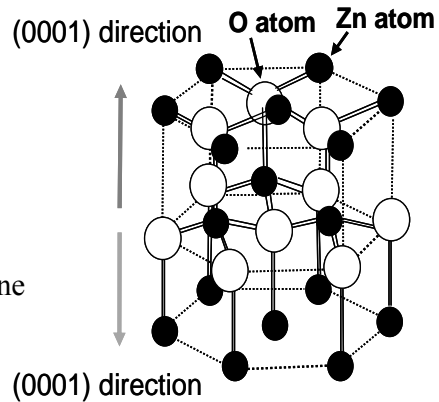
- Transparent material → solar cell

FIGURE A.1 The ZnO crystal structure

A-2. Polarity control

PAMBE(Plasma Assisted Molecular Beam Epitaxy) growth of (Zn-polar (0001) and O-polar (000-1) ZnO by changing the MgO layer thickness. [1-2]

Zn-polar ZnO layer (Zn-face)

Surface is composed of Zn atoms with one dangling bond and three occupied Zn-O bond Zn atoms, forming electropositive centers, tend to bond with electron negative N atoms.

O-polar ZnO layer (O-face)

Surface is composed of O atoms with one dangling bond and three occupied O-Zn bonds. The difference of electron negativity between N and O is small.
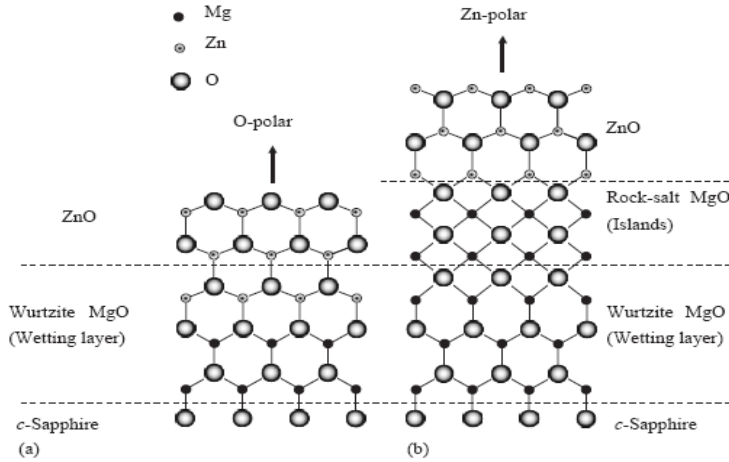
FIGURE A.2 Schematic of atomic arrangement of ZnO on c-plane sapphire with MgO buffer layer thickness (a)O-polar ZnO(t_{MgO} < 3nm) and (b) Zn-polar ZnO (t_{MgO} > 3nm) [1-2]

[1] T. Suzuki, H.J. Ko, A. Setiawan, J.J. Kim, Ko. Saitoh, M. Terauchi, T. Yao, Mater. Scien. Semicon. Processing 6 (2003) 519

[2] H. Kato, M. Sano, K. Miyamoto, T. Yao, J. Cry.. Growth 275 (2005) e2459

감사의 글

CURRICULUMVITAE

PERSONAL BRIEF

Name: Last name: <u>**Siyoung**</u>, Family name: <u>**Kim**</u> (金是永, 김시영)

Date of Birth: 26. Aug. 1983

Nationality: Republic of Korea

Sex: Male (single)

Address: 205-103 Dong Sam-Jung APT, Gaya-1 Dong, Jin-ku, Busan, 604-805, Korea

Affiliation: Major of Nano Semiconductor, Korea Maritime University

Position: Master course student, Department of Nano semiconductor

Office Address: Dongsam-dong 1, Youngdo-ku, Busan, 606-791, Korea

Tel: +82-51-410-4833, Fax: +82-51-410-4833

E-mail: siyoung@hhu.ac.kr

EDUCATION

1999. 3 ~ 2002.2

Gae Geum High school, Pusan, Korea

2002. 3 ~ 2008. 2

B.S. in Semiconductor Physics, Korea Maritime University, Korea,

Thesis: 'Optimization of MBE grown ZnSe/ZnTe superlattice structure'

2008. 3 ~ Now

Master course student, Department of Nano Semiconductor, Graduate

school, Korea Maritime University, Korea

MILITARY SERVICE

2003.10～2005.10

Republic of Korea Marine Corps (sergeant discharge)

A CADEMIC ACTIVITIES

2006.03 ～2008.02

Research student in Nano Material and Device Laboratory,

Research Topic: Molecular Beam Epitaxy growth and characterization

of compound semiconductors.

2008.3~2009.2

일반물리학실험 조교 (한국해양대학교 공과대학)

2009.3 ~ 2009.5

Center for Interdisciplinary Research, Tohoku University, Sendai, Japan

Research Topic: Polarity controlled ZnO buffer layer for the separate of

GaN with high quality films

2008. 3 ~ Now

Master course student in Department of Applied Science, Korea Maritime

Univ.

Research Topic: GaN growth by Hydride Vapor Phase Epitaxy and characterization

PUBLICATION

Molecular Beam Epitaxy of GaSb layers on GaAs(001) substrates by using three-step ZnTe buffer layers, W. Lee**, S.Y. Kim**, S.G. Choi, H.C. Lee, S.T. Lee, S.H. Park, T. Yao, J.S. Song, H.J. Ko, J.H. Chang, **Journal of Crystal Growth**, *2007, vol 305, 40-44*

Molecular Beam Epitaxy of GaSb layers on ZnTe/GaAs: Influence of the chemical composition of ZnTe surface. W. Lee**, S.Y. Kim**, J.S. Song, H.J. Ko, T. Yao, Y.R. Cho, H.C. Lee, S.T. Lee, B.H. Koo, J. H. Chang, **Applied Surface Science**, *2008, vol 254, 7728-7732*

GaSb Thin Films Grown on ZnSe/ZnTe Superlattice Buffer Layers, **S.Y. Kim,** W. Lee, M.N. Jung, H.C. Lee, S.T. Lee, Y.R. Cho, J.H. Chang, **Sae Mulli,** *2008. vol. 56, 266*

Impact of ZnTe buffer on the electrical properties of n-type GaSb:Te films **S.Y. Kim**, W. Lee, M.N. Jung, J.H. Chang, A.K. Nyi, H.C. Lee, J.S. Song, D.C. Oh, S.H. Park, T. Yao, **Applied Surface Science,** *2009. vol. 256, 1261-1264*

Thin film growth of GaSb layers by using three-step buffer layers, W. Lee, **S.Y. Kim**, S.G. Choi, H.C. Lee, S.T. Lee, S.H. Park, T. Yao, J.S. Song, H.J. Ko, J.H. Chang, **Journal of the Research Institute of Industrial Technology,** *2007, vol. 24*

A Study on the GaSb Thin Films Grown on ZnSe/ZnTe Superlattice Buffer Layers, **S.Y.Kim,** W. Lee, M.N. Jung, H.C. Lee, S.T. Lee, Y.R. Cho, J.H. Chang , **Journal of the Research Institute of Industrial Technology,** *2008. vol. 25*

PRESENTATIONS IN INTERNATIONAL CONFERENCES

Improvement of the Crystallinity of MBE Grown GaSb Epilayers by Using Three Step $ZnSe_{1-Y}Te_Y$ Buffer Layers, **S.Y. Kim**, W. Lee, S.G. Choi, H.C. Lee, S.T. Lee, J.S. Song, T. Yao, J.H. Chang, (Asia Nano 2006, 2006.11, Pusan in Korea)

Molecular Beam Epitaxial Growth Chalcogen Nanostructures, S.G. Choi, W. Lee, **S.Y. Kim**, J.H. Chang, H.C. Lee, S.T. Lee, Y.R. Cho (Asia Nano 2006, 2006.11, Pusan in Korea)

Investigation of GaSb/ZnTe heterointerface formation W. Lee, **S.Y. Kim**, H.C. Lee, S.T. Lee, T. Yao, J.S. Song, H.J. Ko, J.H. Chang, (The 13th International Conference on Ⅱ-Ⅵ Compounds, 2007. 09, Jeju-island in Korea)

Molecular Beam Epitaxy of ZnSe/ZnTe Superlattice Buffer Layers for the Growth of Antimonides Thin Film, **S.Y. Kim**, W. Lee, M.N. Jung, H.C. Lee, S.T. Lee, J.S. Song, H.J. Ko, T. Yao, J.H. Chang, (The 13th International Conference on Ⅱ-Ⅵ Compounds, 2007. 09, Jeju-island in Korea)

Molecular Beam Epitaxy of GaSb on ZnTe/GaAs – Influence of the chemical composition of ZnTe surface, W. Lee, **S.Y. Kim**, H.C. Lee, S.T. Lee, Y.R. Cho, J.S. Song, H.J. Ko, T. Yao, J.H. Chang, (The 9th International Conference on Atomically controlled Surfaces, Interfaces and Nanosturctures,ACSIN-9 2007.11, Tokyo in Japan)

Molecular Beam Epitaxy of ZnSe/ZnTe Superlattice Buffer Layers for the Growth of GaSb thin Film on GaAs substrate, **S.Y. Kim**, W. Lee, M.N. Jung, H.C. Lee, S.T. Lee, Y.R. Cho, J.S. Song, H.J. Ko, T. Yao, J.H. Chang, (2007년도 한국재료학회,2007.11, 수원)

Enhancement of Hall mobility of Te-doped GaSb films grown on ZnTe buffer layer by Molecular Beam Epitaxy, **S.Y. Kim**, W. Lee, J.Y. Yu, M.N. Jung, S.T. Lee, H.C. Lee, S.H. Park, D.C. Oh, T. Yao, J.H. Chang, (2008년도 한국물리학회, 2008.04, 대전)

Temperature dependent Hall-effect measurement of Molecular Beam Epitaxial grown GaSb:Te thin Films, A.K. Nyi, **S.Y. Kim**, W. Lee, S.H. Park, D.C. Oh, T. Yao, S.T. Lee, H.C. Lee, J.H. Chang, (2008년도 한국물리학회, 2008.04, 대전)

Cathodoluminescence investigation of GaSb thin films grown on ZnTe buffer layer, W. Lee, S.H. Park, **S.Y. Kim**, H.C. Lee, S.T. Lee, J.S. Song, T. Sekiguchi, J.H. Chang, (VASSCAA-4, 2008.10, Matsue in Japan)

The role of ZnTe buffer on the electrical properties of n-type GaSb:Te films, **S.Y. Kim**, W. Lee, A.K. Nyi, D.C. Oh, S.H. Park, H.C. Lee, J.H. Chang, (VASSCAA-4, 2008.10, Matsue in Japan)

CrN을 사용한 GaN 후막의 구조적, 광학적 특성, 장지호, 주미연, 정미나, 조영지, **김시영**, 구지은, 하준석, 이현재, 박승환, 박진섭, Yao Takafumi, (2009년도 한국물리학회, 2009.04, 대전)

AlN template상의 Hydride Vapor Phase Epitaxy를 이용한 GaN 성장 시 중간층의 역할에 관한 연구, 장지호, 조영지, 정미나, 주미연, **김시영**, 구지은, 하준석, 이현재, 박승환, 박진섭, Yao Takafumi, (2009년도 한국물리학회, 2009.04, 대전)

저온 기상성장법으로 성장된 In 도핑 된 ZnO 나노막대 특성, 장지호, 구지은, 정미나, 김광희, **김시영**, 이원재, 하상훈, 조영래, (2009년도 한국물리학회, 2009.04, 대전)

Investigation of Structural Imperfections in m-GaN Films Grown on *m*-plane (1-10) Al_2O_3 Substrates by Using Hydirde Vapor Phase Epitaxy (HVPE): Anti-Phase Domain, Twins, Asymmetrical Wafer Bowing and Crystallinity, H.J. Lee, J.H. Chang, C.K. Kim, **S.Y. Kim**, K. Kayo, K. Fujii, T. Goto, T. Yao, (ICNS-8, 2009.10, Jeju)

Hydride Vapor Phase Epitaxy of GaN Films on ZnO Templates with Various Polarities, **S.Y. Kim**, H.J. Lee, S.H. Park, W. Lee, M.N. Jung, K. Fujii, T. Goto, T. Sekiguchi, J.H. Chang, T. Yao, (ICNS-8, 2009.10, Jeju)

Structural and Optical Properties of Polarity Controlled HVPE Grown GaN on Al_2O_3 (0001) by Using Zn-/O-Polar ZnO Buffer Layer, W. Lee, B. Dierre, **S.Y. Kim**, M.N. Jung, S.H. Park, H.J. Lee, J.H. Chang, T. Yao, T. Sekiguchi, (ICNS-8, 2009.10, Jeju)

REWARD

2007. 04

Awarded an excellent paper prize by the research institute of industrial

Technology in Korea maritime university

2008.04

Awarded an excellent poster presentation award by Korea physics society

EXPERIENCE OF EQUIPMENTS

Molecular Beam Epitaxy (II-VI and III-V systems): Operation and maintenance, Growth of thin films, RHEED analysis

Hydride Vapor Phase Epitaxy (III-Nitride systems): Operation

Vacuum thermal Evaporator: Operation, deposition,

E-beam Evaporator: Operation, deposition

High resolution X-ray diffraction measurement system: Operation, Data analysis

Atomic force microscopy: Operation, Data analysis

Scanning electron microscope: Operation. Data analysis

Photo luminescence: Operation, Data analysis